TWIN CITIES METROPOLITAN AREA GROUNDWATER FLOW MODEL VERSION 3.0

MAY 2014

METROPOLITAN COUNCIL

The Council's mission is to foster efficient and economic growth for a prosperous metropolitan region.

Metropolitan Council Members

Susan Haigh	Chair	Edward Reynoso	District 9
Katie Rodriguez	District 1	Marie McCarthy	District 10
Lona Schreiber	District 2	Sandy Rummel	District 11
Jennifer Munt	District 3	Harry Melander	District 12
Gary Van Eyll	District 4	Richard Kramer	District 13
Steve Elkins	District 5	Jon Commers	District 14
James Brimeyer	District 6	Steven T. Chávez	District 15
Gary L. Cunningham	District 7	Wendy Wulff	District 16
Adam Duininck	District 8		

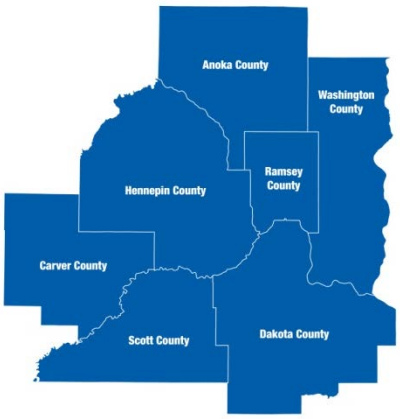

The Metropolitan Council is the regional planning organization for the seven-county Twin Cities area. The Council operates the regional bus and rail system, collects and treats wastewater, coordinates regional water resources, plans and helps fund regional parks, and administers federal funds that provide housing opportunities for low- and moderate-income individuals and families. The 17-member Council board is appointed by and serves at the pleasure of the governor.

This publication printed on recycled paper.

On request, this publication will be made available in alternative formats to people with disabilities. Call Metropolitan Council information at 651-602-1140 or TTY 651-291-0904.

About this Report

The Metropolitan Council recognizes that water supply planning is an integral component of long-term regional and local comprehensive planning. The Council has implemented a number of projects to provide a base of technical information needed to make sound water supply decisions.

This report summarizes the result of work to update the regional groundwater flow model, which meets the requirements of Minn. Stat., Sec. 473.1565 calling for the Council to engage in planning activities which must include “development and maintenance of a base of technical information needed for sound water supply decisions including surface and groundwater availability analyses, water demand projections, water withdrawal and use impact analyses, modeling, and similar studies”.

The report is organized into six major sections. The introduction provides an overview of the Council and the need for the project. The next five sections discuss methods and results.

Special funding for this project was provided through the Clean Water Fund.

Prepared By

This report was prepared by Barr Engineering Co. in cooperation with the Metropolitan Council.

Project principles and managers include:

Ray Wuolo, P.E., P.G., Barr Engineering Co.

Tim Brown, formerly of Barr Engineering Co.

Evan Christianson, P.G., Barr Engineering Co.

I hereby certify that this report was prepared by me or under my direct supervision and I am a duly Licensed Professional Geologist under the laws of the state of Minnesota.

Evan Christianson

_____Evan G. Christianson

Date: ____May 30, 2014___ Reg. No. 51379

Recommended Citation

Metropolitan Council. 2014. Twin Cities Metropolitan Area Regional Groundwater Flow Model, Version 3.0. Prepared by Barr Engineering. Metropolitan Council: Saint Paul, MN.

Acknowledgements

The Council would like to acknowledge the following people who graciously shared their time and expertise to assist with this study and its resulting recommendations:

Dave Welter, Managing Partner Computational Water Resource Engineering (3rd Party Reviewer)

Randal Barnes, Ph.D., University of Minnesota (Technical Advisory Group attendee)

Kelton Barr, P.G., Braun Intertec (Technical Advisory Group attendee)

Glen Champion, P.G., MN Department of Natural Resources (Technical Advisory Group attendee)

Mark Collins, HDR (Technical Advisory Group attendee)

Amal Djerrarri, P.E., Ph.D., MN Department of Health (Technical Advisory Group attendee)

Perry Jones, P.G., U.S. Geological Survey (Technical Advisory Group attendee)

Bob Karls, Antea Group (Technical Advisory Group attendee)

Kerry Keen, University of Wisconsin (Technical Advisory Group attendee)

Adam Kessler, P.G., HDR (Technical Advisory Group attendee)

Joy Loughry, P.G., MN Department of Health (Technical Advisory Group attendee)

Paul Lucas, Antea Group (Technical Advisory Group attendee)

Trisha Moore, University of Minnesota – SAFL (Technical Advisory Group attendee)

Ole Olmanson, P.G., Shakopee Mdewakanton Sioux Community (Technical Advisory Group attendee)

Bill Olsen, M.S., Dakota County (Technical Advisory Group attendee)

John Oswald, P.G., LBG (Technical Advisory Group attendee)

Jeremy Rivord, P.G., MN Department of Natural Resources (Technical Advisory Group attendee)

Brennon Schaefer, MN Department of Agriculture (Technical Advisory Group attendee)

Erik Smith, U.S. Geological Survey (Technical Advisory Group attendee)

Andrew Streitz, P.G., MN Pollution Control Agency (Technical Advisory Group attendee)

Robert Tipping, P.G., PhD, MN Geological Survey (Technical Advisory Group attendee)

Princesa VanBuren Hansen, P.E., MN Department of Natural Resources (Technical Advisory Group attendee)

Jim Westerman, City of Woodbury (Technical Advisory Group attendee)

Table of Contents

List of Tables

List of Figures

List of Appendices

Abbreviations and Acronyms

BFI	BaseFlow Index
Ce	Eau Claire Formation
Cj	Jordan Sandstone
Cms	Mt. Simon Sandstone
Csl	St. Lawrence Formation
Ctc	Tunnel City Group
Cw	Wonewoc Sandstone
CWI	County Well Index
DNR	Department of Natural Resources
EDA	Environmental Data Access
GB	Gigabyte
GHB	General Head Boundary package/boundary
GIS	Geographical Information System
GUI	Graphical User Interface
Ku	Cretaceous
LIDAR	Light Detection and Ranging
MNW	Multi-Node Well package/boundary
MODFLOW	modular finite-difference ground-water flow model
MPCA	Minnesota Pollution Control Agency
NAD	North American Datum
NED	National Elevation Dataset
NLCD	National Land Cover Database
NWIS	National Water Information System
ObWell	DNR Observation Well
Op	Prairie du Chien Group
Os	St. Peter Sandstone
PEST	Parameter Estimation software
Qu	Quaternary
RAM	Random Access Memory
RCH	Recharge package/boundary
RIV	River package/boundary
RSME	Root Mean Square Error
RVOB	River Observation Package
SWB	Soil Water Balance model
SWUDS	State Water Use Data System
USGS	U.S. Geological Survey
UTM	Universal Transverse Mercator
UZF	Unsaturated-Zone Flow
WEL	Well package/boundary

1.0 Introduction

Groundwater-flow models have been a part of regional water-supply planning in the Twin Cities for several decades (e.g. Schoenberg and Guswa, 1982; Young, 1992; Hansen and Seaberg, 2000; Metropolitan Council, 2009) and have evolved with modeling technologies and our understanding of the hydrogeologic system of the region. The Minnesota Pollution Control Agency (MPCA) developed a regional analytic element groundwater-flow model in the 1990s that is commonly referred to as the "Metro Model" or "Metro Model 1". In 2007 the Metropolitan Council (Council) contracted with Barr Engineering Co. to develop and calibrate a regional groundwater-flow model of the Twin Cities region to assist the Council with regional water-supply planning. This model used many of the datasets that were developed as part of the Metro Model 1 but employs a different modeling code and therefore, was given the name "Metro Model 2". The Metro Model 2 went through one minor revision phase and was subsequently released as Metro Model 2.1. The model was designed to help address a broad range of regional planning questions and to be as flexible as practical in order to accommodate new questions or scenarios, while still incorporating the best available data. Some examples of questions the model is intended to help address include:

- Given projected water demands, what impacts may be expected on groundwater levels and groundwater-dependent surface-water features?
- What combinations of source aquifers, well locations, and withdrawal rates can be used to achieve sustainable water consumption?

The use of the Metro Model 2.1 has been a fundamental part of the Council's water-supply planning efforts and supports the Metropolitan Area Master Water Supply Plan. Implementation of the Metropolitan Area Master Water Supply Plan includes regular updates of the Metro Model as new water-supply planning questions are developed and new information becomes available.

While Metro Model 2.1 provides a quantitative tool for the Council's regional water-supply planning work, certain model limitations hinder its ability to fully answer questions about impacts to surface-water features and the seasonal (transient) impacts of groundwater withdrawals. Metro Model 2.1 uses the modeling code MODFLOW-96 which is considered a legacy code and is no longer supported by the U.S. Geological Survey (USGS). Also, numerous hydrogeological studies have been completed for the Twin Cities metro area

since the construction of the Metro Model 2.1, much of it accelerated by the passage of the 2008 Clean Water, Land and Legacy Amendment to the Minnesota Constitution. Data from these studies have refined our understanding of the extent and properties of aquifers in the metro area and have provided data that can be used to help reduce uncertainty in model predictions.

To achieve the Council's legislative mandate to maintain a base of technical information necessary for sound water-supply decisions, the Metro Model 2.1 needed to be updated to include the newly acquired information. This update also provides an opportunity to expand the model domain in order to consider the effects of growth in counties beyond the seven-county metro area and to add transient capability to model predictions. This information will support metropolitan area communities as they begin their next round of local comprehensive planning, including water-supply planning, expected to begin in 2015.

Update of the Metro Model is occurring in three phases:

- Phase 1: Recharge model update.
- Phase 2: Conceptual groundwater model update.
- Phase 3. Model calibration.

This report describes the results of Phase 2 and 3: conceptual groundwater model update and model calibration. Results of Phase 1, recharge model update, are presented in Appendix A.

1.1 Purpose & Objectives of the Metro Model

The overarching objective of this effort is to maintain a groundwater-flow model that allows the Council and land use and water utility planners across the metropolitan area to consider both groundwater availability and land use during the planning processes. The model was developed and calibrated for the primary purpose of predicting the effects of current and future groundwater withdrawals and land use on groundwater levels and the base flows of streams at a regional scale. These types of model predictions are useful for interpreting hydrogeologic data, informing future data collection, and for evaluating alternatives to enhance sustainable use of water resources in the metropolitan area.

Benefits of this revision of the Metro Model include: 1) incorporation of new information, 2) implementation of newer and better-supported software, 3) enhanced methods to

understand parameter sensitivities and uncertainty in model predictions, 4) improved representation of Quaternary unconsolidated sediments and their influence on the groundwater-flow system, 5) the ability to simulate seasonal effects of climatic and pumping stresses, and 6) an expanded model domain.

1.2 Changes from Metro Model 2.1

This update of the Metro Model includes the following changes:

- Expansion of the model domain from the seven-county metropolitan area to the eleven counties in and around the Twin Cities area;
- Addition of transient simulation capabilities in which temporal variations in aquifer stresses (e.g., pumping rates) and changes in aquifer storage are accounted for;
- Inclusion of new geologic mapping information;
- Inclusion of up-to-date pumping data (i.e. data through 2011);
- Consideration of new groundwater-level information;
- Inclusion of additional rivers in the new model domain, and minor revision of some rivers in the Metro Model 2.1 model domain;
- Revisions to model boundary conditions resulting from expansion of the model domain;
- Revisions to hydrostratigraphic units in model layers;
- A new approach to defining aquifer properties in model cells representing Quaternary deposits;
- A new approach to capturing the effect of secondary porosity/permeability features near the bedrock contact with overlying Quaternary deposits;
- Inclusion of confining characteristics of some hydrostratigraphic units;
- A new approach for distinguishing the difference between infiltration of water below the root zone and groundwater recharge at the water table; and
- Use of the newly released MODFLOW-NWT instead of MODFLOW-96, which, among other attributes, provides for a much more stable and reproducible means of accounting for changes in saturated-unsaturated conditions.

2.0 Hydrogeologic Setting & Conceptual Model

The conceptual hydrogeologic model is a schematic description of how water enters, flows, and leaves the groundwater system. Its purpose is to define the major sources and sinks of water, the division or lumping of hydrostratigraphic units into aquifers and aquitards, the direction of groundwater flow, the interflow of groundwater between aquifers, and the interflow of water between surface waters and groundwater. The conceptual hydrogeologic model is scale-dependent (i.e., local conditions may not be identical to regional conditions) and will vary depending upon the purpose of the groundwater-flow model. It is important to recognize that the conceptual hydrogeologic model for the Metro Model was developed with the understanding that the primary purpose of the Metro Model is to predict the effects of current and future groundwater withdrawals and land use on groundwater levels and the base flows of streams at a regional scale. While this conceptual hydrogeologic model may be applicable to a variety of other problems and scales for which a groundwater-flow model has predictive utility, the model user is responsible for evaluating the validity of the conceptual hydrogeologic model for those problems and scales.

2.1 Study Area Location

This updated conceptual hydrogeologic model of regional groundwater flow is focused on the eleven-county Twin Cities metropolitan area located in east-central Minnesota and encompassing Anoka, Carver, Chisago, Dakota, Hennepin, Isanti, Ramsey, Scott, Sherburne, Washington, and Wright counties. The understanding of the general geologic setting of the metro area has not changed substantially since the Metro Model 2.1 was constructed, but the expansion of the model domain and recent geologic mapping has introduced some new geologic units into the model. The following section describes the general geologic setting of the updated model domain.

2.2 Geologic Setting

Sedimentary rocks deposited during the Paleozoic Era and unconsolidated sediments deposited in association with glaciations during the Quaternary Period comprise the dominant aquifers in the metro area. Large epicontinental seas flooded much of the North American craton during the Paleozoic Era. All of the Paleozoic sedimentary rocks of importance for this study were deposited in the Hollandale Embayment (Figure 1); a shallow shelf that extended from southeastern Minnesota and western Wisconsin southward to Iowa and Illinois (Austin, 1969). The water level in the sea fluctuated, thereby causing

transgressions (a rising of sea level) and regressions (a dropping of sea level), resulting in a sequence of different sedimentary rocks (e.g., limestone, shale, and sandstone). These sequences, which are distinguishable and mappable over large areas, have been given formal names and are described further in Section 2.2.1. At a large regional scale, these bedrock units are often grouped together and referred to as the Cambrian-Ordovician aquifer system (Young, 1992) (Figure 1).

Numerous smaller geologic structures are present within the Hollandale Embayment. During the middle- to late-Ordovician Period, additional tectonic activity resulted in faulting and folding of existing sedimentary rocks and the formation of the Twin Cities basin, centered near Minneapolis (Figure 1) and the Galena Basin, along the Minnesota and Iowa border (Mossler, 2008). Large fault zones were reactivated along the western and eastern boundary of the Mesoproterzoic Midcontinent rift (Mossler, 2011). Faulting is likely present along the entire perimeter of the Twin Cities basin but faults are difficult to map where subsurface data are sparse and the displacement of bedrock units in some areas may be small (Mossler, 2011). The presence of these fault zones has become more definitive with the collection of additional subsurface data and it is now possible to map their locations and offsets in many areas of the metro area (Figure 2). The most extensive faulting is in southeastern Washington County, northeastern Dakota County, western Scott County, and western Carver County (Figure 2). Major fault zones in these areas include the Cottage Grove and Hastings fault zones along the eastern side of the Twin Cities basin, the Douglas fault and Pine fault zones along the northern and northwestern sides of the basin, and the Belle Plaine fault along the southwestern side of the basin (Mossler and Chandler, 2009, Mossler, 2011, Runkel and Mossler, 2006, Mossler and Tipping, 2000). Along these fault zones, bedrock units may be offset by hundreds of feet.

During the Cretaceous Period, another shallow epicontinental sea covered the western interior of North America, resulting in a sequence of shale, siltstone, sandstone, and some carbonates that overlie Paleozoic rocks along the western and southwestern part of the Hollandale Embayment in Minnesota (Mossler, 2008).

After deposition of the Paleozoic bedrock, a long period of erosion occurred, resulting in large bedrock valleys and the removal and/or dissection of bedrock units. Subsequent glaciations during the Quaternary Period resulted in additional erosion of bedrock formations. Deep valleys were incised into the bedrock units across the Twin Cities area

(Figure 3), severing some bedrock units entirely. Much of the paleo-bedrock surface was subsequently covered by the deposition of thick sequences of glacial till and outwash during the Quaternary Period.

2.2.1 Hydrostratigraphy

Geologic units underlying the Twin Cities metropolitan area fall into four broad categories: (1) Precambrian volcanic and crystalline rocks; (2) Precambrian through Ordovician sedimentary rocks; (3) Cretaceous sedimentary rocks; and (4) Quaternary unconsolidated deposits. The Precambrian volcanic and crystalline rocks generally are not considered major water-bearing units and are at a considerable depth below ground surface throughout most of the metropolitan area. The Precambrian through Ordovician sedimentary rocks make up the major regional aquifers and aquitards in the metropolitan area and include units such as the Hinckley Sandstone, the St. Lawrence Formation, and the Prairie du Chien Group. A stratigraphic column of these sedimentary rocks from Mossler, (2008) is provided in Appendix F. The Cretaceous sedimentary rocks comprise a minor aquifer and local aquitards in the far western metropolitan area. The Quaternary unconsolidated deposits include glacial outwash, glacial till, and alluvial deposits and serve as localized aquifers and aquitards throughout the metropolitan area.

Runkel and others (2003a;b), in their comprehensive review and compilation of hydrogeologic data for Paleozoic bedrock in southeastern Minnesota, describe the importance of secondary porosity features in defining the hydrogeologic characteristics of aquifers and aquitards. They note that individual lithologic units have very different hydrogeologic characteristics in near-surface settings compared to deep bedrock conditions. Secondary porosity (i.e. systematic fractures, dissolution features, and nonsystematic fractures) is prevalent within 200 feet of the bedrock surface. Where a lithologic unit is greater than 200 feet below the bedrock surface, secondary porosity features are generally less abundant. These secondary porosity features typically result in increased hydraulic conductivity and a greater range in hydraulic conductivity for shallow bedrock conditions. The 200-foot depth cutoff used by Runkel and others (2003a) is also used below to describe deep versus shallow bedrock conditions for the hydrostratigraphic units pertinent to this study, with the recognition that the change in hydrogeologic characteristics is transitional and does not necessarily take place at a defined depth.

2.2.1.1 Basal Aquitard

The lowermost confining unit in the study area is comprised of several Precambrian lithostratigraphic units. These units extend to great depth (up to several kilometers) and the hydraulic characteristics of these units are poorly known. While in some areas the basal aquitard may supply water to wells, they are regionally considered an aquitard (Delin and Woodward, 1984). Along the axis of the Hollandale Embayment, Middle Proterozoic sedimentary, volcanic, and mafic intrusive rocks associated with the Midcontinent rift system comprise the basal aquitard. These Middle Proterozoic rocks include the Fond du Lac and Solor Church Formations across much of the Twin Cities basin and southeastern Minnesota. It should be noted that the Hinckley Sandstone, also associated with the Midcontinent rift system, is not considered part of the basal aquitard and is grouped with the Mt. Simon Sandstone as the Mt. Simon-Hinckley aquifer (discussed below). In the western portion of the model domain Proterozoic and Archean igneous and metamorphic rocks form the basal aquitard.

2.2.1.2 Mt. Simon – Hinckley Aquifer

The Mt. Simon – Hinckley aquifer consists of the Mt. Simon Sandstone and the Hinckley Sandstone. The Hinckley Sandstone comprises the uppermost Precambrian bedrock in the study area. It is a quartzose sandstone and is distinct from the underlying Solor Church and Fond du Lac Formations. The lower portion of the Hinckley Sandstone has shale and siltstone layers and a saprolith is present at the top of the Hinckley Sandstone in some areas. The Hinckley Sandstone may not be easily distinguished from the overlying Mt. Simon Sandstone.

The Cambrian Mt. Simon Sandstone is chiefly a medium- to coarse-grained, quartzose sandstone. However, particularly in the upper part of the unit, beds of finer grained shale and siltstone are present (Mossler, 2008; Runkel and others, 2003a). The unit ranges in thickness from less than 25 feet up to 375 feet in far southeast Minnesota. In the Twin Cities basin the Mt. Simon Sandstone is about 200 feet thick (Mossler, 2008). Runkel and others (2003a) divide the unit into a lower coarse clastic component, and an upper fine clastic component. Fine clastic beds in the upper portion of the unit have low permeability may provide hydraulic confinement (Runkel and others, 2003a). At the local scale, the unit may be distinguished into two or more hydrostratigraphic units. However, given limited knowledge regarding the extent and competence of confining beds within the unit, at the

regional scale of this study the Mt. Simon Sandstone is combined with the Hinckley Sandstone as one hydrostratigraphic unit.

The hydraulic conductivity of the Mt. Simon Sandstone is typically greater where the unit is near the bedrock surface. Runkel and others (2003a) calculated the average hydraulic conductivity of the Mt. Simon Sandstone for deep bedrock conditions to be 21 ft/day based on specific-capacity tests. Large-scale aquifer tests and packer tests indicate a range from 0.38 to 17 ft/day (Runkel and others, 2003a;b). The fine clastic beds in the upper part of the Mt. Simon Sandstone may have hydraulic conductivities on the order of 10^{-2} to 10^{-4} ft/day. For shallow bedrock conditions, Runkel and others (2003a;b) calculated the average hydraulic conductivity to be 29.3 ft/day with a range of 1 to 70 ft/day. The difference in hydraulic conductivities for deep versus shallow bedrock conditions likely reflects a more densely developed fracture network where the unit is near the surface. At greater depth, the Mt. Simon sandstone is commonly assumed to have few fractures and dissolution features; however, this assumption remains unproven (Runkel and others, 2003a).

The Mt. Simon – Hinckley aquifer was heavily used as a water supply in the past, but there have been recent efforts to reduce the amount of water withdrawn from the aquifer. During the 1970's and 1980's, storage within the aquifer was being depleted due to high rates of pumping from the aquifer. As a result, Minnesota Statues Section 103G.271 Subdivision 4a now prohibits the allocation of new water appropriation permits for the aquifer unless no practical alternatives are available. The statute also restricts allocations for potable use only. In the Twin Cities, a large cone of depression exists within the Mt. Simon – Hinckley aquifer (Delin and Woodward, 1984; Sanocki and others., 2009) (Figure 4).

2.2.1.3 Eau Claire Aquitard

The Cambrian Eau Claire Formation is a low-permeability unit that overlies the Mt. Simon-Hinckley aquifer and acts as a regional aquitard, limiting leakage between the Mt. Simon – Hinckley aquifer and the overlying aquifer system. The Eau Claire Formation is a combination of siltstone, very fine feldspathic sandstone, and greenish-gray shale. Some of the shale beds may be as thick as several feet (Mossler and Tipping, 2000). The Eau Claire Formation thins northward, with a maximum thickness of over 200 feet near the Iowa border and decreasing to less than 100-feet thick in the Twin Cities basin (Mossler, 2008).

The hydraulic conductivity of the Eau Claire Formation is typically several orders of magnitude lower for deep bedrock conditions compared to shallow bedrock conditions. Horizontal hydraulic conductivities for deep bedrock conditions have been measured on the order of 10^{-2} to 10^{-3} ft/day and vertical conductivities of 10^{-4} ft/day (Runkel and others, 2003a). Logged cores and borehole videos indicate that secondary pores are rare for deep bedrock conditions (Runkel and others, 2003a;b). In shallow bedrock conditions where secondary porosity features are most extensive, the Eau Claire Formation can yield water to wells and could be classified as an aquifer. The majority of wells that are open to the Eau Claire Formation are located where the unit is the uppermost bedrock, primarily in the northern part of the metro area and along the St Croix and Mississippi rivers. Based on specific-capacity data, the hydraulic conductivity of the Eau Claire Formation in shallow bedrock conditions ranges from less than 1 ft/day to as much as 100 ft/day, with an average of 36.7 ft/day (Runkel and others, 2003a).

2.2.1.4 Wonewoc Aquifer

The Cambrian Wonewoc Sandstone is typically a medium to coarse-grained, cross-stratified quartzose sandstone with moderately high permeability. The unit conformably overlies the Eau Claire Formation and is considered an aquifer. It is divided into two major lithofacies, which are difficult to differentiate: the Ironton and Galesville Sandstones. These lithofacies were formally recognized as formations but are now classified as members (Mossler, 2008). A third lithofacies, the Mill Street Conglomerate, is only present at the northern extent of the Wonewoc and is not explicitly simulated in the model.

The hydraulic conductivity of the Wonewoc aquifer varies, depending on its depth. For deep bedrock conditions, the hydraulic conductivity ranges from 1 to 31 ft/day (Runkel and others, 2003a) with values of several feet per day being typical (Runkel and others, 2003b). Based on specific-capacity tests, the hydraulic conductive of the Wonewoc aquifer for shallow conditions ranges from less than 1 to 60 ft/day, with an average value of 26.8 ft/day (Runkel and others, 2003a).

Historically the Wonewoc aquifer has not been highly utilized in the central metro area because sufficient water supplies can be obtained from shallower units, such as the Prairie du Chien and Jordan aquifers. Recently, the Wonewoc aquifer (and the overlying Tunnel City aquifer) has undergone greater evaluation by the Minnesota Geological Survey, particularly in the northwest metropolitan area where the Prairie Du Chien and Jordan

aquifers are absent (Runkel and others, 2003b). Because the Wonewoc and Tunnel City are the uppermost bedrock units in the northwest metropolitan area, they are more highly fractured and thus more permeable. Conversely, where these units are overlain by other bedrock units (e.g., the St. Lawrence Formation), the fracturing is less developed and the ability to produce usable quantities of water is substantially reduced.

2.2.1.5 Tunnel City Aquifer and Aquitard

The Cambrian Tunnel City Group is often lumped together with the Wonewoc Sandstone or is lumped together with the overlying St. Lawrence Formation as a regional aquitard (for example, Delin and Woodward, 1984). For this study, the unit is treated as a single hydrostratigraphic unit. The Tunnel City Group, formerly known as the Franconia Formation, refers to rock between the Wonewoc Sandstone and the St. Lawrence Formation and consists of three formations: the Lone Rock Formation, the Davis Formation, and the Mazomanie Formation (Mossler, 2008).

The Lone Rock Formation is a low-permeability, very fine- to fine-grained sandstone with minor thin beds of shale and dolostone, while the Mazomanie Formation is comprised of coarser sandstone and possesses greater primary permeability. The Davis Formation has limited extent and has only been mapped in Faribault and Freeborn Counties of Minnesota (outside the model domain) (Mossler, 2008). The Lone Rock Formation makes up nearly all of the Tunnel City Group in the southern half of the model domain. The coarser Mazomanie Formation is present in the northern half of the model domain with a thickness of 10 to 20 feet in west-central Hennepin County and up to 115 feet in Chisago County (Mossler, 2008). The Mazomanie Formation constitutes greater than 20 percent of the Tunnel City Group in parts of Anoka, Chisago, Hennepin, Isanti, Ramsey, Sherburne, Washington, and Wright Counties (Runkel and others, 2003a). In western Wisconsin, the Mazomanie Formation is the principal lithostratigraphic unit of the Tunnel City Group (Mossler, 2008).

At a local scale, the Tunnel City Group can be treated as two units: an upper aquifer unit comprised of the Mazomanie Formation (for areas where the unit is near the bedrock surface) and a lower confining unit comprised of the Tunnel City Group where it is deeply buried) (Runkel and others, 2003a). For the scale of this study, the unit is combined but is intended to be parameterized in a way to represent the regional differences in the hydraulic character of the group. Where the Mazomanie Formation comprises a significant part of the Tunnel City Group, particularly in the north and east metro area, the hydraulic conductivity

for deep bedrock conditions ranges from less than 1 ft/day to 65 ft/day, with an average hydraulic conductivity of 27.8 ft/day; for shallow bedrock conditions hydraulic conductivity ranges from less than 1 ft/day to 75 ft/day with an average of 31.7 ft/day (Runkel and others, 2003b). Where the Mazomanie Formation is not present, hydraulic conductivity of the Tunnel City Group for deep bedrock conditions ranges from less than 1 ft/day to 10 ft/day with an average of 5.9 ft/day and hydraulic conductivity for shallow bedrock conditions ranges from and less than 1 ft/day to 40 ft/day with an average of 32.3 ft/day (Runkel and others, 2003b).

2.2.1.6 St. Lawrence Aquitard and Aquifer

The St. Lawrence Formation is a regional leaky aquitard that separates the Tunnel City Group from the overlying Jordan aquifer. The unit consists of fossiliferous, silty to very fine crystalline dolostone, interlayered with thin intervals of siltstone and in some areas, very fine-grained glauconitic sandstone and shale (Mossler and Tipping, 2000). Across most of southeast Minnesota, the lower part of this unit is dominated by carbonate rock while the upper part of the unit is mostly siltstone and very fine-grained sandstone (Runkel and others, 2003b). Near the St. Croix River valley, the St. Lawrence Formation consists almost entirely of siltstone (Runkel and others, 2003a; Mossler, 2008).

Runkel and others (2003b and 2006) describe the St. Lawrence Formation as having low bulk hydraulic conductivity in the vertical direction, which can provide confinement. These confining characteristics are present where the St. Lawrence Formation is relatively deep and overlain by the Jordan Sandstone. The bulk vertical hydraulic conductivity of the St. Lawrence Formation was measured between 10^{-5} to 10^{-4} ft/day in Ramsey County (Runkel and others, 2003a). The horizontal hydraulic conductivity of the St. Lawrence Formation for deep bedrock conditions has been measured in the range of less than 1 ft/day to 50 ft/day. Runkel and others (2003a) attribute these relatively high horizontal hydraulic conductivity values to interconnected bedding plane fractures and dissolution cavities.

Where the St. Lawrence Formation is at shallow depth, it may not act as a confining unit over significant geographic extent. In these areas, interconnecting fractures result in relatively high bulk hydraulic conductivity values and the unit can act as a relatively high-yielding aquifer. Some discrete intervals or beds within the unit can provide confinement locally if interconnected fractures and other secondary porosity features are minimally developed. Based on specific-capacity test data the horizontal hydraulic conductivity of the

St. Lawrence Formation for shallow bedrock conditions typically ranges from less than 1 ft/day to 75 ft/day with an average of 46 ft/day (Runkel and others, 2003b)

2.2.1.7 Jordan Aquifer

The Cambrian Jordan Sandstone consists of several coarsening-upward sequences. The sequences consist of two distinguishable facies: (1) medium- to coarse-grained, cross-bedded, friable quartz sandstone, and (2) a massive, very fine-grained, typically bioturbated, feldspathic sandstone, with some siltstone and shale (Mossler and Tipping, 2000). Typically, the lower 5 to 50 feet of the unit consists of the finer grained feldspathic facies and the upper 50 to 80 feet consists of the coarser grained quartzose facies (Runkel and others, 2003a). However, in many areas the two facies can be intercalated (Mossler, 2008).

Groundwater flow in the Jordan Sandstone is commonly assumed to be primarily intergranular, but secondary permeability undoubtedly develops due to jointing and differential cementation (Schoenberg, 1990). Runkel and others (2003a) note that flow along fractures within the Jordan Sandstone should be expected in shallow bedrock conditions and fracture flow may take place locally for deep bedrock conditions. Results from standard pumping tests indicate that the hydraulic conductivity of the Jordan Sandstone ranges from 0.1 to 100 ft/day with an average value of 48.5 ft/day (Runkel and others, 2003a). Hydraulic conductivity values measured from specific-capacity tests for deep bedrock conditions indicate a range of less than 1 to 35 ft/day with an average of 17.4 ft/day. For shallow bedrock, hydraulic conductivity values ranges between less than 1 to 95 ft/day with an average of 43.3 ft/day (Runkel and others, 2003a). The extent and thickness of the coarser-grained lithofacies and the development of secondary porosity are suspected to be the main factors influencing the range of hydraulic conductivity for this unit. Runkel and others (2003) note that where the finer grained lithofacies is present at the top of the Jordan Sandstone, the facies can be grouped with the overlying Oneota Formation and acts as a confining unit. Where the finer-grained lithofacies are at the base of the Jordan Sandstone, the facies may be grouped with the underlying St. Lawrence Formation and act as an aquitard.

2.2.1.8 Prairie du Chien Group Aquifer

The Ordovician Prairie du Chien Group is comprised of the Shakopee Formation (upper) and the Oneota Dolomite (lower). The Shakopee Formation is a dolostone with interbedded, thin layers of fine- to medium-grained quartz sandstone and shale. The Oneota Dolomite is

commonly massive- to thick-bedded dolostone. The lower part of the Oneota Dolomite can be oolitic or sandy. Both formations are locally karsted and the upper contact may be rubbly (from pre-aerial exposure) (Mossler and Tipping, 2000).

Flow in the Prairie du Chien Group is dominated by three to five relatively thin (5 to 10 feet thick) zones of highly connected horizontal fractures in the Shakopee Formation and the upper part of the Oneota Dolomite (Runkel and others, 2003a). The horizontal hydraulic conductivity of the Prairie du Chien Group can range over nine or more orders of magnitude (Runkel and others, 2003a). Within thin, highly fractured zones, hydraulic conductivity can exceed 1,000 ft/day. Between these fracture zones, the hydraulic conductivity is much lower but has not been studied extensively because most wells are open to the more-productive, highly fractured zones. Based on specific-capacity tests, the hydraulic conductivity of the Prairie du Chien Group for deep bedrock conditions ranges from less than 1 to 50 ft/day with an average of 33.5 ft/day. In shallow bedrock conditions, hydraulic conductivity values typically ranges from less than 1 to 125 ft/day with an average value of 60.8 ft/day, or about double compared to deep bedrock conditions (Runkel and others, 2003a). Standard pumping tests have measured the hydraulic conductivity of the Prairie du Chien Group ranging from 0.1 ft/day to 163 ft/day, with most of the high hydraulic conductivity values measured for wells screened primarily in the Shakopee Formation (Runkel and others, 2003a).

Runkel and others (2003a) demonstrated that the lower portion of the Oneota Dolomite is massive, of low permeability, relatively unfractured, and acts as a regional aquitard that separates the permeable portions of the Prairie du Chien Group (the upper part of the Oneota Dolomite and the Shakopee Formation) from the Jordan Sandstone. Vertical hydraulic conductivity for the Oneota Dolomite has been measured as low as 10^{-4} ft/day. For this study, the two formations are grouped into one hydrostratigraphic unit; the Prairie du Chien Group aquifer. Parameterization within the Prairie du Chien Group aquifer is intended to allow for relatively high horizontal hydraulic conductivity, representing discrete beds that allow significant horizontal movement of water and relatively low vertical hydraulic conductivity, representing the confining characteristics of the Oneota Dolomite.

2.2.1.9 St. Peter Aquifer

The Ordovician St. Peter Sandstone is divided into two members. The upper Tonti Member is very fine- to medium-grained quartzose sandstone that is generally massively to very

thickly bedded. The lower Pigs Eye Member is an interbedded sandstone, siltstone and shale (Mossler, 2008). The Tonti Member is extensive and present over the entire extent of the St. Peter Sandstone in Minnesota. The Tonti Member's thickness ranges from 100 to 120 feet. The Pigs Eye Member is less extensive; it is 40-65 feet in the metro area and along the unit's western subcrop, southwest of the Twin Cities (Runkel and others, 2003a; Mossler, 2008). To the east and south, the Pigs Eye Member is thinner; generally 2-5 feet thick (Mossler, 2008).

The lower Pigs Eye Member typically has low vertical permeability and functions as an aquitard that overlies the Prairie du Chien Group (Palen, 1990, Runkel and others, 2003a). The upper Tonti Member has much greater permeability and functions as an aquifer. The hydraulic conductivity of the St. Peter Sandstone typically ranges between 2 and 50 ft/day for deep bedrock conditions and between 1 and 74 ft/day for shallow bedrock conditions. The greater hydraulic conductivity values for shallow bedrock conditions are indicative of the influence of secondary porosity features (Runkel and others, 2003a).

2.2.1.10 Glenwood, Platteville, and Decorah Aquitard

The Glenwood, Platteville, and Decorah Formations are grouped into a single hydrostratigraphic unit for this study. The Glenwood Formation is a blocky shale with thin stringers of fine- to coarse-grained quartz sandstone. The Platteville Formation is a fossiliferous limestone and dolomite. The Decorah Shale is the uppermost Paleozoic bedrock present in the Twin Cities area and consists of calcareous shale with some thin beds of limestone. These units have a limited extent within the model area. They are present in southeast Hennepin County, Ramsey County, western Washington County, smaller areas of Dakota County, and in Rice and Goodhue counties along the southern edge of the model domain.

The Decorah Shale, Platteville Formation, and Glenwood Formation are typically together considered a regional aquitard (Kanivetsky, 1978). However, some highly fractured portions of these units supply domestic wells, and a number of springs originate from the units. Recent work by Anderson and others (2011) and Runkel and others (2011) classify the Platteville Formation as a hybrid unit (both aquifer and aquitard). The unit can act as a competent aquitard, restricting vertical flow. However, well-developed macropore and fracture networks along discrete intervals, particularly in shallow bedrock conditions, result in relatively high horizontal hydraulic conductivities. Anderson and others (2011) noted that

measured hydraulic conductivity values for the Platteville Formation range over eight orders of magnitude, from less than $1x10^{-4}$ to more than $1x10^{4}$ ft/day.

Due to the limited extent of these units, the recognition that groundwater flow within the units is typically under perched conditions and separate from the regional groundwater system (Anderson and others, 2011, Runkel and others, 2003), the need to keep the groundwater-flow model computationally efficient necessitates that they are numerically combined with overlying Quaternary sediments in the groundwater-flow model. This combining is described in Section 3.4.2.

2.2.1.11 Cretaceous Aquifer

The Cretaceous aquifer is of limited extent - generally present in discontinuous swaths in the far western metropolitan area. The unit is up to 200 feet thick in parts of Stearns and McLeod Counties and is composed of poorly cemented sandstone, siltstone, and shale of the Dakota Formation and unnamed sedimentary rocks. The Dakota Formation consists of a very fine- to coarse-grained, angular to subangular sandstone. The unnamed sedimentary rocks consist of calcareous yellow-gray to pale olive to pale red sandstone, siltstone, shale, and claystone. It is typically difficult to distinguish Dakota Sandstone from weathered Paleozoic rock and the clayey saprolith which is considered to be widely present in the western metropolitan area (Minnesota Geological Survey, 2009; 2012). The age of these rocks is unknown and may be either Lower to Upper Cretaceous or Late Paleozoic.

Cretaceous bedrock was not included in the previous version of the Metro Model. Recent mapping and expansion of the model domain allow this unit to be included. The hydraulic characteristics of the unit are not well known. The Dakota Formation is extensively used as an aquifer in Iowa and other Cretaceous deposits are used as aquifers in southwestern Minnesota. These rocks are thought to be hydrologically distinct from the overlying glacial till and underlying Paleozoic and or Precambrian rocks and are therefore considered separately in this study.

2.2.1.12 Quaternary Aquifers and Aquitards

Quaternary deposits of glacial till, sand, gravel, clay, and silt cover the bedrock surface over the majority of the study area and range in thickness from 0 to over 600 feet. These Quaternary deposits are the result of the advance and retreat of large continental ice sheets over and near the Twin Cities metro area over the past two-million years. Glacial till was

deposited underneath and adjacent to the glaciers. Glacial meltwater rivers deposited sand and gravel (outwash). Ice blocks were left in place to melt as the glaciers retreated, forming kettle lakes. As the glaciers retreated, meltwater rivers incised through the glacial deposits and into the bedrock units. These rivers also deposited thick sequences of sand and gravel (outwash). Upon glacial re-advancement, these river channels were often filled with new sediments forming buried bedrock valleys. In other areas, large glacial lakes formed where glacial meltwater was unable to drain away. Thick deposits of fine-grained sediment formed along the bottom of these lakes. Near the end of the last glaciations, the ancestral Mississippi River and the River Warren (ancestral Minnesota River) incised back into the glacial deposits, forming wide river valleys with alluvial terrace deposits and backwater areas.

Quaternary sediments are highly heterogeneous. At the scale of the eleven-county metropolitan area it is impractical to lump Quaternary deposits into hydrostratigraphic zones based on their provenance. Rather than pursue a geologic delineation of the lateral and vertical extent of unconsolidated aquifers and aquitards, this report utilized a study conducted by Tipping (2011), which mapped textural characteristics of the Quaternary sediments in the eleven-county metropolitan area and correlated those textures to representative ranges in hydraulic conductivity values. Use of this data is further described in Section 3.5.2.

2.2.2 Groundwater Levels and Flow Directions

Groundwater-level measurements are available from several different sources, all with varying degrees of accuracy. Since the last update of the Metro Model in 2009, additional data have been collected. These include: regional and local synoptic water-level measurements, mapping of potentiometric surfaces as part of county and regional hydrogeologic assessments, additional Minnesota Department of Natural Resources (DNR) observation-well data, and new static-water levels tabulated in the County Well Index.

Several regional and local synoptic water-level datasets have recently been developed. These data provide a “snap-shot” of water levels in an aquifer over a large area and are generally considered very accurate in both elevation and horizontal location. The USGS conducted two rounds of data collection in March 2008 and August 2008 across the seven-county metro area (Sanocki and others, 2009). These data supplement synoptic water-level measurements performed in 1988 and 1989 (Andrews and others, 1995) and offer insight

into seasonal and long-term water-level trends in the regional aquifers. Additional synoptic measurements were made near White Bear Lake in 2011 and 2012.

In addition to the synoptic water-level data, new observation wells maintained by the DNR have been installed to supplement existing wells. These observation wells provide a high-fidelity record of trends in groundwater levels and are typically measured on a monthly basis. Some of these observation wells have been recently outfitted with data loggers to record data several times per day. There are a number of other dedicated monitoring wells that are not part of the Minnesota DNR network. These include wells at contaminated sites, watershed organization monitoring networks, and some municipal water supplier monitoring wells. The data from these wells are generally very reliable and are measured anywhere from yearly to weekly.

Water levels are also typically measured as part of well installations and are recorded in the County Well Index. These data are typically less reliable but are well-distributed across the entire study area. Details on how water-level data are incorporated into the model are presented in the model calibration section (Section 4.1.1 Hydraulic Head).

Groundwater flows from zones of high piezometric head to low piezometric head. In the metro area, groundwater flow in the upper aquifer units is towards the major rivers (Sanocki and others, 2009; Delin and Woodward, 1984). Regionally, groundwater flow in the deeper Mt. Simon – Hinckley aquifer is towards the major rivers, as well. However, locally within the Mt. Simon – Hinckley aquifer there is a large cone of depression in south eastern Hennepin County where groundwater flows towards the center of the cone of depression, eventually discharging via pumping wells (Sanocki and others, 2009) (Figure 4). Locally, around high capacity wells or well fields, smaller cones of depression may also develop in the upper bedrock or Quaternary aquifers, resulting in local groundwater-flow paths directed to high-capacity wells.

2.2.3 Infiltration and Recharge

The source of nearly all of the water in the metro area's aquifers is from infiltrating precipitation. The amount of direct precipitation that is able to infiltrate at land surface and move below the root zone is the maximum amount of water available to recharge the underlying aquifers. This amount is dependent upon the rate and duration of precipitation, the soil type and soil cover, land use, evapotranspiration, and topography.

The portion of infiltration that moves from the unsaturated sediment below the root zone into underlying aquifers has been estimated in a variety of ways. Norvitch and others (1973) estimated that this rate is between 4 and 10 inches per year. Schoenberg (1990) estimated that the annual groundwater flow to streams, which is assumed to approximately equal groundwater recharge, is equivalent to 1.60 to 4.30 inches per year, with an average of 4.07 inches per year. Lorenz and Delin (2007), using a regional regression method, estimated the average annual recharge rate to surficial materials in the Twin Cities area to range between 3 and 9 inches per year. Metropolitan Council (2012; Appendix A) estimated infiltration of water below the root zone using the Soil Water Balance (SWB) model for the Twin Cities metropolitan area for climatic and land use data from 1988-2011. The SWB model estimated infiltration on a 90 meter-square grid. The aerial average infiltration for the period 1988-2011 was 8.2 inches per year and ranged between 2.7 and 13.0 inches per year.

Infiltration estimated by the SWB model is similar, but considered different, than groundwater recharge. The most important distinction between infiltration and groundwater recharge is the time lag between infiltration of water past the root zone and recharge at the water table. In additional, small-scale processes such a local flow systems and rejection of infiltration due to a high water table often result in differences between recharge and infiltration. Further discussion of how infiltration from the SWB model is incorporated in the MODFLOW model is presented in Section 3.6.1

2.2.4 Regional Discharge

In the Twin Cities area, groundwater flows toward the major discharge zones of the Mississippi, Minnesota, and St. Croix Rivers. Local discharge to the gaining portions of smaller streams and tributaries can also take place within the surficial aquifers.

Groundwater-inflow rates into smaller streams can be estimated from stream-flow gauging records. Baseflow conditions (i.e., the groundwater component of stream flow) typically accounts for most of the flow during the winter months, when runoff is small. On an annual average, approximately 15 to 25 percent of total flow in streams results from groundwater discharge into the streams (Schoenberg, 1990).

Various attempts have been made to estimate groundwater inflows into the large rivers in the Twin Cities by detailed gauging of river flows. The most recent efforts were performed by

the U.S. Geological Survey, which used sophisticated Doppler measurement techniques to calculate flows in the rivers at several cross sections. In principle, by subtracting the stream flows measured at an upstream section from the stream flows measured at a downstream section (and assuming no tributary inflows), the difference in stream flow should be attributable to base flow from groundwater. In smaller streams, this technique works reasonably well but in large streams, such as the Minnesota and Mississippi Rivers, the error in the measurement is nearly equal to or greater than the calculated groundwater inflows – rendering the calculated baseflows highly suspect.

The other major source of groundwater discharge in the Twin Cities area is through pumping wells. Most of the suburban communities obtain their water supply from high capacity wells. For some aquifers in the Twin Cities area, such as the Mt. Simon – Hinckley aquifer, discharge from wells makes up a significant amount of the total discharge from the aquifer.

3.0 Model Construction

3.1 MODFLOW

MODFLOW simulates three-dimensional, steady-state and transient groundwater flow (saturated) using finite-difference approximations of the partial differential equation of groundwater flow:

$$\frac{\partial}{\partial x}\left(K_{xx}\frac{\partial h}{\partial x}\right)+\frac{\partial}{\partial y}\left(K_{yy}\frac{\partial h}{\partial y}\right)+\frac{\partial}{\partial z}\left(K_{zz}\frac{\partial h}{\partial z}\right)-W=S_s\frac{\partial h}{\partial t}$$

where:

K_{xx}, K_{yy}, and K_{zz}: are the three principal directions of the hydraulic conductivity tensor
W: sources and sinks
S_s: specific storage
h: hydraulic head
t: time

MODFLOW was developed by the U.S. Geological Survey and is in the public domain. It is widely used and accepted. The version of MODFLOW used for this model is MODFLOW-NWT (Niswonger and others, 2011).

3.2 Computing Requirements

MODFLOW can be download for free from the USGS website at: http://water.usgs.gov/nrp/gwsoftware/modflow.html. The MODFLOW files produced for this project will run on any Windows machine (Windows 7 or newer recommended). The model is known to run well on a Windows 7 machine with 16 GB of RAM and a 2.8 GHz quad-core processor (note: the model only needs one processor core). Tests of a machine with only 2GB of RAM failed. It is suspected that at least 4GB of RAM are necessary. At least 10 GB of hard disk space should be available to save the model output files. Large transient model runs may take a significant about of time to run (over 24 hours); steady-state model runs should complete in under 15 minutes.

To view model results or modify the input files, a graphical user interface (GUI) is recommended, but not necessary. The model was constructed using Groundwater Vistas (ver. 6.55 build 6, 64-bit), however, much of the calibration was set up outside of a GUI. There are a number of other GUI's available (some for free and some for a considerable

cost). Any reputable GUI should be able to read the native MODFLOW files. Instructions for importing model files into several popular GUIs are provided in the user manual and tutorials associated with this report.

3.3 Model Domain

The model domain covers an area of 8,350 square miles, encompassing the entire eleven-county Twin Cities metro area (Figure 5). The domain was chosen to include the area of interest (eleven-county metro area) and to extend far enough beyond that area in order to minimize the effects of artificial boundary conditions within the area of interest. To the east, the model extends into Wisconsin to account for groundwater flow into the St. Croix River from the east. To the northwest and west, the model extends beyond the edge of the Mt. Simon-Hinckley aquifer. To the south, the model extends into Goodhue, Le Sueur, and Rice Counties. The model domain was defined using minor watershed boundaries, reflecting a growing connection between the management of groundwater and surface water resources. Using watershed boundaries better allows for Metro Model 3 results to be mapped with surface water information.

3.3.1 Model Layering and Discretization

The model domain is subdivided into rectilinear grid cells in order to solve the finite-difference approximations. The model is divided laterally into 410 rows and 340 columns using a regular grid with cells sizes of 500 meters x 500 meters. Vertically, the model is divided into nine layers using a deformed model layer approach where layer elevations generally correspond with hydrostratigraphic units (Figure 6). Of 1,254,600 model cells, 778,806 are active and used in the computational process.

The length unit of the model is meters and site coordinates are in UTM NAD 83, Zone 15N. The X offset of the model grid origin is 369,875 meters and the Y offset for the origin is 4,883,875 meters. The time unit for the model is days.

Between each model layer is a quasi-3D layer (McDonald and Harbaugh, 1988; Harbaugh, 2005). Quasi-3D layers are used in the calculation of vertical conductance between model cells but are not explicitly simulated; the only effect of quasi-3D layers is to restrict the vertical flow between model cells, heads are not calculated for quasi-3D layers (Harbaugh, 2005). Quasi-3D layers are used to represent the confining characteristics of the base of the St. Peter Sandstone, Prairie du Chien Group, and Tunnel City Group, where

present. Because these units may be represented in different model layers due to faulting (see discussion on faults below), quasi-3D layers were set up between each model layer. Each quasi-3D confining layer is set at a constant thickness of 0.1 meters. This thickness is set for convenience in computation of the conductance and does not represent the actual thickness of confining beds. Where confining units are present the vertical hydraulic conductivity of the quasi-3D layer is set low, and adjusted during calibration, to reduce the conductance between layers (refer to Figure 7 through Figure 17 for distribution of hydrostratigraphic units). Where confining units are not present the vertical hydraulic conductivity was set at 10,000 m/day so that the quasi-3D layer has no significant effect on the conductance between layers.

Table 1. General model hydrostratigraphic layers

Layer Number[1]	Hydrostratigraphic Unit
1-9	Quaternary sediments[2] and Glenwood-Platteville-Decorah aquitard
4-9	Cretaceous aquifer[3]
2	St. Peter aquifer
3	Prairie du Chien Group aquifer
4	Jordan aquifer
5	St. Lawrence aquitard and aquifer
6	Tunnel City Group aquifer and aquitard
7	Wonewoc aquifer
8	Eau Claire aquitard
9	Mt. Simon and Hinckley aquifer

[1] The layer numbers for each hydrostratigraphic unit do not follow this convention in faulted area.
[2] These units may occupy more than one layer where lower hydrostratigraphic units are not present.
[3] May overlie several units and occupy several layers.

General model layer assignments for each hydrostratigraphic unit are shown in Table 1. In areas where the upper bedrock units are not present, the Quaternary sediments can be represented by more than one model layer. For example, in areas where the Jordan Sandstone is the first bedrock unit present (i.e., the St. Peter Sandstone and Prairie du Chien Group are not present) the Quaternary occupies model Layers 1-3. The Cretaceous aquifer sedimentary rocks overlie several of the bedrock units in the western portion of the model. Model cells representing these sedimentary units may occupy more than one layer depending on the thickness of the unit. Typically, model cells representing these units are overlain by several layers representing the Quaternary sediments (Figure 6).

Offsets in the bedrock as a result of faulting were handled in two ways. For major faults in southwestern Scott County, western Carver County, southeastern Washington County, and

northeastern Dakota County, hydrostratigraphic units are offset to different model layers in the area of faulting (i.e., at the location of the fault there is an inhomogeneity or change in the hydraulic conductivity within the model layer) (see Figure 2 and Figure 6). For other smaller faults, or those not as well defined (i.e., in northwestern Hennepin County), the model layers were interpolated across the faulted zone and the hydrostratigraphic unit remains within its "normal" model layer.

Raster grids were developed for the top of each hydrostratigraphic unit within the model domain. Data were compiled from several sources in order to obtain a complete coverage for the entire model domain for each unit. Data sources used are shown in Appendix E . Stratigraphy data from well-drilling records in the County Well Index (CWI) were used to determine the elevation of the lithologic contacts in areas outside the study areas listed in Appendix E. Several of the data sets listed in Appendix E were developed at different times and at different scales. It is common for the datasets to be inconsistent in areas of overlap or at the edges of two studies (e.g., county boundaries). In general, more recent studies were assumed to be correct at locations with inconsistencies. Where discrepancies arise at the edges of two separate studies, the elevations and extent of bedrock units were manually adjusted to provide a smoother and more continuous dataset. Model-layer elevations on the Minnesota side of the St. Croix and Mississippi Rivers were extended across the river valleys into Wisconsin.

The extent and elevations of the top of each hydrostratigraphic unit in the model are shown on Figures 7 to 16. A composite of the bedrock unit extents is shown on Figure 17.

3.4 Stress Periods and Time Steps

The model was developed and calibrated for both transient and steady-state use. Steady-state models are time-constant, meaning stresses on the aquifer system (e.g. pumping and recharge) are fixed with respect to time and the aquifer is simulated to be at equilibrium to those stresses. Transient models are time-variant, meaning stresses change over time and the aquifer is not at an equilibrium state. Water can go into or be released by aquifer storage in a transient model. Aquifer storage is not a component of a steady-state model.

The steady-state model produced for this study represents a period of 2003-2011. Pumping and recharge for the steady-state model are average rates for that period.

For transient calibration, a model representing a period of 2007-2011 with monthly stress periods and weekly time steps was used. Recharge and pumping in the transient model change monthly and a solution for aquifer head and flow is calculated on a weekly basis. The initial conditions for this transient model were generated by a steady-state model representing average 2003-2005 conditions; this steady-state model is intended only for use during calibration.

A much longer transient model representing 1995-2011 was developed after calibration. Monthly stress periods and weekly time steps were also used for the longer transient simulation. Recharge and pumping change monthly and a head solution is calculated on a weekly basis. This model is too computationally intensive to use during calibration. Results from the 1995-2011 transient simulation may be useful for assessing long-term impacts and to assess the ability of the model to capture long-term transient head change (see Section 5.0).

3.5 Aquifer Properties

Aquifer properties of hydraulic conductivity (vertical and horizontal) and storage (specific yield and specific storage) are assigned to each active model cell by interpolating values between pilot points (Doherty and others, 2010) for bedrock hydrostratigraphic units or effective values for Quaternary sediments. Each of these approaches is described in detail below. Aquifer properties were based on data available in the Minnesota Department of Health (MDH) aquifer test database and from the Minnesota Geological Survey (Tipping, 2011) at the time of model construction. It is recognized that some existing data was not included in the database, and a multi-agency workgroup has been formed to support MDH efforts to more effectively compile and share aquifer test data.

3.5.1 Hydraulic Conductivity of Bedrock Hydrostratigraphic Units

As mentioned in Section 2.2.1 and described in detail by Runkel and others (2003a), the bulk hydraulic conductivity of aquifers and aquitards in southeastern Minnesota is controlled by both primary hydraulic conductivity (matrix permeability) and secondary hydraulic conductivity (systematic fractures, dissolution features, and nonsystematic fractures). To capture these two main components of the bulk hydraulic conductivity, the method described below and illustrated on Figure 18 was employed to determine input for MODFLOW.

The primary hydraulic conductivity was estimated using pilot points (Doherty and others, 2010). Pilot points were distributed evenly across each hydrostratigraphic unit to allow for relatively smooth interpolated distributions. Pilot points were not tied to measurements of hydraulic conductivity; measured hydraulic conductivity/transmissivity were used as observations (Section 4.1.4). The number of pilot points used for each unit varied depending on existing data for the unit (pumping tests, hydraulic head measurements) and the areal extent of the unit. Where more data are available more parameters are justified and where the extent of a unit is large more pilot points are needed to allow for spatial variability across the model domain. Twenty pilot points were used to define the primary hydraulic conductivity for the Prairie du Chien Group and Jordan Sandstone. Only three pilot points were used for the Cretaceous aquifer due to limited constraining data and limited areal extent of the unit. For each of the other bedrock hydrostratigraphic units, 15 pilot points were used. Values of both primary horizontal hydraulic conductivity (K_{px}) and vertical anisotropy ($\frac{K_{bx}}{K_{bz}}$) at each pilot point were set as adjustable parameters for model calibration as described in Section 4.2.1. Ordinary kriging was used to interpolate the primary hydraulic conductivity between pilot points for each hydrostratigraphic unit. The location of and values of individual pilot points are shown on Figure 54 through Figure 74 and discussed in Section 4.4.2.

A depth-dependent function was used to increase the hydraulic conductivity values for individual units where they are near the top of bedrock surface. Features controlling secondary hydraulic conductivity are known to be present at all depths but are most prevalent within 200 feet of the top of bedrock surface (Runkel and others 2003a).

The depth dependent function allows for increased values of hydraulic conductivity in areas where features controlling secondary hydraulic conductivity are prevalent (i.e. the unit is near the bedrock surface). The function used is shown in Equation 3-1.

$$D = C * \left(10^{-\lambda d}\right) + 1 \qquad \text{(Eqn. 3-1)}$$

where:
D = scaling factor used to determine total hydraulic conductivity
C = constant used to control the max value of D
λ = constant used to control max depth (d) at which D is greater than 1
d = depth of unit below bedrock surface

To determine the bulk hydraulic conductivity for input to MODFLOW, equations 3-2 and 3-3 were used on a cell-by-cell basis for horizontal and vertical hydraulic conductivity respectively.

$$K_{bx} = K_{px} * D \qquad \text{(Eqn. 3-2)}$$

$$K_{bz} = \frac{K_{bx}}{K_{bz}} * K_{bx} \qquad \text{(Eqn. 3-3)}$$

where:
K_{bx} = bulk horizontal hydraulic conductivity used as input for MODFLOW
K_{bz} = bulk vertical hydraulic conductivity used as input for MODFLOW
K_{px} = primary horizontal hydraulic conductivity
($\frac{K_{bx}}{K_{bz}}$) = vertical anisotropy ratio
D = scaling factor determined with Eqn. 3-1

For model calibration, values of *C* and λ, used in Equation 3-1, for each hydrostratigraphic unit were set as adjustable parameters.

3.5.2 Hydraulic Conductivity of Quaternary Glenwood, Platteville, and Decorah Hydrostratigraphic Units

The hydraulic conductivity values assigned for model cells representing the Quaternary, Glenwood, Platteville, and Decorah hydrostratigraphic units were determined using methods similar to Anderman and Hill (2000) and also discussed in Anderson and Woessner (1992, pg 69). Effective hydraulic conductivities were calculated for each model cell based on material type and thickness (e.g., sand, clay, Platteville Formation) within each model cell. The type, extent, and thickness of Quaternary sediments in the eleven-county metropolitan area were determined from mapping conducted by Tipping (2011).

The material types classified by Tipping (2011) are mapped as a matrix of points spaced 250 meters (820 feet) apart in the horizontal direction and 6.1 meters (20 feet) apart in the vertical direction. The point data set from Tipping (2011) was converted to a series of raster grids, each representing material types along a single elevation (each elevation raster was spaced 20 feet apart). The MODFLOW grid was constructed such that each of the model cells (which are 500 m x 500 m in size) encompasses four of the material-type raster cells (each representing 250 m x 250 m) (see Figure 19). In order to distinguish between MODFLOW model cells and the material-type raster cells, the material-type raster cells are

referred to as material type “voxels” throughout the rest of this report and are illustrated in Figure 19.

A series of external processing scripts was developed to determine the thickness of each material type and to calculate the effective horizontal and vertical hydraulic conductivities for each material-type voxel that intersects a MODFLOW cell. The general process is as follows.

1) The thicknesses of each material type that intersects a MODFLOW cell ($b_{i,j,g}$) were determined using the bottom of the MODFLOW cell and the minimum of either the top of the MODFLOW cell or the water table (only saturated thicknesses were used to determine the effective hydraulic conductivities). The water-table elevations used for these calculations are based on the regional water-table surface as developed by Barr Engineering (2010). The water-table elevation dataset developed by Barr Engineering (2010) was extended to cover the entire model domain using interpolated water-level data from CWI. Similar to Barr Engineering (2010), surface-water features were not included in the development of the water-table surface to reduce the potential effect of perched water bodies.
2) Effective horizontal hydraulic conductivities for each material type voxel ($Kx)_{i,j}$ were determined using Eq. 3-4 (Anderson and Woessner, 1992). The horizontal hydraulic conductivity value applied to the MODFLOW cells is the arithmetic mean of the effective horizontal hydraulic conductivity for each of four material-type voxels that intersect each MODFLOW cell (see Figure 19)

$$(K_x)_{i,j} = \sum_{g=1}^{m} \frac{Kx_{i,j,g}\, b_{i,j,g}}{B_{i,j}} \quad \text{(Eqn. 3-4)}$$

$$B_{i,j} = \sum_{g=1}^{m} b_{i,j,g} \quad \text{(Eqn. 3-5)}$$

where:
$B_{i,j}$ is the thickness of a model cell
$b_{i,j,g}$ is the thickness of an individual material type
$Kx_{i,j,g}$ is the horizontal hydraulic conductivity of an individual material type

3) Effective vertical hydraulic conductivities for each material type voxel $(Kz)_{i,j}$ were determined using Eq. 3-6 (Anderson and Woessner, 1992). The vertical hydraulic conductivity value applied to the MODFLOW cells is the harmonic mean of the effective vertical hydraulic conductivity for each of four material-type voxels that intersect each MODFLOW cell.

$$(K_z)_{i,j} = \frac{B_{i,j}}{\sum_{g=1}^{m} \frac{b_{i,j,g}}{Kz_{i,j,g}}} \quad \text{(Eqn. 3-6)}$$

where:
$B_{i,j}$ is the thickness of a model cell
$b_{i,j,g}$ is the thickness of an individual material type
$Kz_{i,j,g}$ is the vertical hydraulic conductivity of an individual material type

3.5.3 Storage Coefficients

Storage coefficients (specific storage and specific yield) are necessary parameters in transient simulations. Similar to primary hydraulic conductivity, pilot points were used to define storage coefficients. The location and number of pilot points used to define storage coefficients is identical to those locations used for hydraulic conductivity. The upper-bound limit for specific yield assigned to Quaternary sediments in the calibration process was 0.42. Johnson (1963) and Cohen (1963) report typical maximum specific yield values for silts, sands, and gravels in the 0.35-0.42 range, based on drainage characteristics in the laboratory and field studies.

3.6 Boundary Conditions

Boundary conditions establish the sources and sinks of water for a groundwater-flow model. The geologic and hydrogeologic conceptual models aid in the selection of the appropriate boundary conditions. Boundaries used for this study are described below.

3.6.1 Recharge/Infiltration

The SWB model (Dripps and Bradbury, 2007) was used to estimate monthly infiltration rates (flux of water below the root zone) for a regular grid of 90 meter x 90 meter cells for the years 1988-2011 (see Appendix A). The SWB model calculates infiltration based on methods similar to Thornthwaite (1948) and Thornthwaite and Mather (1957) and is implemented using GIS data for soil type, land use, climate, and topography.

The difference between the SWB model grid size and the MODFLOW model grid size required some preprocessing of the SWB model output prior to incorporation into MODFLOW. The following process was used:

1) A GIS shapefile of the MODFLOW grid was intersected with the SWB output to obtain the area of intersection of each SWB model cell to each MODFLOW model cell
2) For each MODFLOW cell the area weighted average infiltration was calculated using the values of each SWB cell and the area of intersection associated with a given cell.
3) During model calibration infiltration grids were scaled depending on parameters associated with land use and soil type combinations as described in Section 4.2.6 prior to calculating the area weighted average infiltration for each MODFLOW cell.

Infiltration values from SWB were then used in conjunction with the Unsaturated-Zone Flow (UZF) package to simulate recharge in MODFLOW. The UZF package (Niswonger and others, 2006) simulates water flow and storage in the unsaturated zone using a kinematic wave approximation to Richards' Equation (Smith, 1983; Smith and Hebbert, 1983; Niswonger and others, 2006) and is a substitute for the commonly used recharge and evapotranspiration packages of MODFLOW. For this study, the evapotranspiration components of the UZF package were not used, as evapotranspiration is considered in the simulation of infiltration with the SWB model.

The primary purpose of using the UZF package rather than the recharge package is to allow for the time lag between infiltration below the root zone and recharge to the water table to be accounted for during transient simulations. The UZF package also allows for recharge volumes to be rejected from the model where the water table is simulated at the top of the model (ground surface) and/or reduced if permeability of unsaturated sediments is low and unable to transmit specified infiltration volumes. Because the SWB model does not consider the depth of the water table, the ability to reject infiltration with the UZF package may be important in areas where the water table is near the surface (i.e. large wetland complexes, particularly in regional groundwater discharge zones such as the Minnesota River Valley). Also, the SWB model only considers permeability of surficial soils; deeper unsaturated sediments may not be able to transmit as much water as the surficial soils.

The UZF package has three main input parameters. These include vertical hydraulic conductivity of the unsaturated zone, the Brooks-Corey epsilon of the unsaturated zone, and

the saturated water content of the unsaturated zone. The effective vertical hydraulic conductivity of the unsaturated zone is calculated in the same way as vertical hydraulic conductivity of the saturated zone described in Section 3.5.2, except only sediments between the groundwater surface and water table are considered in the calculation. The Brooks-Corey epsilon was set at a constant representative value of 3.0 for all model cells. The Brooks-Corey epsilon typically ranges between 2.5 to 4.1 for unconsolidated sediments (Rawls and others, 1982; Brooks Corey, 1964) but data are insufficient for further refinement at the scale of the model. The saturated water content was set at a representative value 0.25 for all model cells based on a typical porosity.

Implementing the full UZF package significantly increased model run times for the transient model to the point of limiting the ability to calibrate the model. A significant "spin-up" simulation period is necessary to properly account for lag time between infiltration and recharge and to allow for soil moisture in the unsaturated zone to reach proper levels prior to the period of calibration. Also, small changes in the thickness of the saturated zone made the model very non-linear and difficult to solve as wetting fronts from infiltrated water migrate to the water table. To overcome this limitation for transient simulations, a simplified two-layer model was designed to use the UZF package to capture the time lag between infiltration and recharge. The full model was then run with the recharge package (RCH), applying recharge directly to the water table as calculated using the UZF package of the simple model.

The general process of implementing the simple model to calculate recharge time lags is outlined below:

1). The full steady-state model is run and the thickness of the unsaturated zone is calculated.

2.) A simple two layer model is run. Layer 1 of the two-layer model represents the unsaturated zone and is essentially dry. Layer 2 consists of constant head cells with head values defined from results of the steady-state model. Monthly infiltration rates from the SWB model for January, 1988 to December, 2011 are used as input to the two-layer model. The UZF package of the two-layer model tracks wetting fronts and soil moisture through the unsaturated zone and calculates recharge rates and timing at the water table. An initial test with a shorter spin-up time (2000-2006) was tested but was

found to be insufficient. So, the entire infiltration time-series from SWB was used, resulting in a spin-up period of 1988 to 2006.

4.) The full transient model is run with recharge calculated by the two-layer model for January, 2007 to December, 2011 applied directly to the water table with the recharge package, thus dramatically decreasing total run times.

Figure 20 shows examples of the difference between recharge and infiltration for several different areas of the model domain. Areas with a high permeability unsaturated zone and shallow water table, such as central Anoka County, show little difference in timing and magnitude between infiltration and recharge. In central Carver County, an area with a deeper water table and lower permeability unsaturated zone, the recharge signal is very muted when compared to infiltration. Other areas, such as central Dakota County, and central Washington County, show a slightly muted recharge signal and an obvious time lag between peak rates of infiltration and peak rates of recharge.

3.6.2 No-Flow Boundaries

No-flow boundaries were set for all cells outside the model domain but within the finite-difference grid; these cells are not included in computations. For the northern and western edges of the active model domain, where the aquifer units thin and pinch out, no-flow boundaries were used (see Figure 5 for the location of these boundaries). No-flow boundaries were also used along the southwestern edge of the model domain, representing an approximate groundwater-flow path toward the Minnesota River (Delin and Woodward, 1984; Young, 1992) (as shown on Figure 5). No-flow boundaries also define the base of the model (bottom of Layer 9), which typically corresponds with the bottom of the Mt. Simon-Hinckley aquifer and the top of the regional basal aquitard.

3.6.3 General Head Boundary

The southern extent of the model domain does not coincide with a physical hydraulic boundary and it is known that groundwater flows across this boundary (Delin and Woodward, 1984). To simulate groundwater flux into or out of the model, the General Head Boundary (GHB) package was used along the southern edge of the model domain (shown on Figure 5). The GHB boundary condition is a Cauchy Condition type of head-dependent boundary and simulates groundwater flux into or out of the model domain that is driven, in part, by a reference head that is fixed at a specified distance from the boundary. This allows

for more realistic simulation of changes in boundary flux due to pumping stresses than when using no-flow or constant-head boundaries. Reference-head values assigned to the GHB cells in the model are based on piezometric surface contours in Delin and Woodward (1984). Although the contours in Delin and Woodward (1984) were interpreted from water-level measurements made between 1970 and 1980, a comparison to more recent water-level data in the County Well Index (CWI) suggests that they adequately represent current conditions.

Head values were manually assigned to groups of GHB cells by interpolating the Delin and Woodward (1984) contours at a distance of up to 25 km perpendicular to the model boundary. The 25 km distance was chosen because it provides sufficient separation from the model boundary to minimize boundary effects and is in the vicinity of a prominent regional groundwater divide. In areas of the model boundary where a groundwater divide or constant-head source is present less than 25 km from the model boundary, the distance to the divide or constant head was specified. For example, GHB cells in the vicinity of the Zumbro River in Layer 1 were assigned a distance value equal to the distance between the cell and the river. Head values defined for the GHB cells are constant and do no vary during the transient simulations.

The following assumptions were made during assignment of GHB reference heads and distances in model layers that were either 1) not contoured in Delin and Woodward (1984) or 2) combined with other model layers in their aquifers:

- GHB cells in Layer 1, which includes the Quaternary and Upper Carbonate aquifers, were assigned reference heads based on water-table contours from country geologic atlas data and interpolations of CWI data.
- GHB cells beyond the outcrop extent of the St. Peter Sandstone (Layer 2) were assigned the same reference head and distance values assigned to the corresponding cells in Layer 1.
- The Tunnel City Group (formerly the Franconia Formation) is classified as an aquitard by Delin and Woodward (1984). It is currently considered to be part of an aquifer with the Wonewoc Sandstone (formerly Ironton and Galesville Sandstones). GHB cells in the model layer representing the Tunnel City aquifer (Layer 5) were assigned the same reference head and distance values as the corresponding cells in the Wonewoc aquifer (Layer 6).

- GHB cells in aquitard layers (Layer 5: St. Lawrence, Layer 8: Eau Claire) were assigned the average reference head and distance values of the adjacent aquifer layers above and below the unit.

3.6.4 Constant-Head Boundaries

Constant-head boundaries were assigned to the eastern edge of the model domain (see Figure 5). Values for the constant head cells were derived from results of a groundwater-flow model for Pierce, Polk, and St. Croix counties, Wisconsin (Juckem, 2009). The Wisconsin model is a three-layer model that groups the Quaternary sediments and the upper bedrock aquifers above the Eau Claire Formation into a single model layer. The head values from this Wisconsin model layer were assumed to reasonably represent the actual potentiometric surface and were applied as the constant-head values for model Layers 1-7 of the Metro Model. The Eau Claire Formation and the Mt. Simon Sandstone are simulated as individual layers in the Wisconsin model and hence heads from those layers were used to define the constant head values for Layers 8 and 9. All constant-head boundaries remain fixed during the transient simulations.

3.6.5 Surface-Water Features

Rivers, streams, and lakes were simulated using the river (RIV) boundary. Determining the number of surface-water features to simulate in the model is typically a tradeoff between simulating a network of surface-water features dense enough to represent groundwater discharge and recharge associated with those features and a network that is so dense that it causes the water table to be almost entirely constrained by imposed boundary conditions. The intended use of the model and other available data also dictate the density of surface-water features simulated. For example, the intended use of this model necessitated including all designated trout streams as well as the ability to synchronize the surface-water features simulated using the SWB recharge model with inputs to MODFLOW.

Major rivers and streams simulated in the model are shown on Figure 21. Simulated rivers within the extent of the previous version of the Metro Model have remained mostly the same except the simulated portions of some trout streams were updated based on newer Minnesota DNR data. Also, Cedar Creek in Anoka County was added to better represent groundwater flow in the surficial sediments in that area. Outside the extent of the previous Metro Model, major rivers and stream were added. These include: Buffalo Creek, Chub Creek, Clearwater River, High Island Creek, Le Sueur Creek, Rush River, Snake River, and

St Francis River. Many smaller streams and tributaries to those listed above were also added but are too numerous to list here. All rivers simulated in the model area are included in GIS data supporting this report. Only perennial portions of these streams, as defined in the National Hydrological Dataset, were included. To incorporate these rivers and streams into the model, a GIS shapefile was created with each river, or stream, divided into several reaches. Reaches were first divided at stream gauge locations and then at points where a break in slope was observed by viewing a digital elevation model and USGS topographic maps, or where dramatic changes in stream width were observed on aerial imagery. The beginning and end of each reach, or line segment, was assigned a stage elevation based on average stream gage data, a 10 meter National Elevation Dataset (NED) elevation model data (USGS, 2009), or LIDAR data, if available. Average stream-gauge data was compiled as part of the Metro Model 2 construction from the USGS, Army Corps of Engineers, and local government agencies. Groundwater Vistas was used to interpolate between the endpoints of each reach to assign river stage values for model cells between the endpoints.

All open-water bodies simulated in the SWB recharge model were included in the MODFLOW model. These include all open-water bodies as mapped in the USGS 2006 National Land Cover Database (NLCD). The SWB recharge model does not calculate a recharge value for open-water bodies. To account for leakage from these water bodies to the groundwater system and to provide a more robust connection between the SWB recharge model and MODFLOW, all open water bodies were simulated using the river boundaries.

The inclusion of all open-water bodies simulated in SWB presents several challenges when integrating to the larger grid dimensions of MODFLOW. The SWB model uses a grid that is 90 m x 90 m in size; significantly smaller than the 500 m x 500 m MODFLOW grid. It is common for more than one surface-water feature to intersect a model cell. These surface-water features may be either lakes or streams, and likely have different stage values. A representative stage was calculated for the model cells following methods similar to Feinstein and others (2010). In general, for model cells with multiple surface-water features, if a stream or riverine lake is present within a model cell, then the stage assigned to the RIV boundary is the stage of the stream. For model cells containing only open-water bodies (lakes, but not rivers or streams), the stage is set at the conductance-weighted average stage of all water bodies intersecting the cell. Effectively, the water body that encompasses most of a model cell will generally have a larger influence on the stage assigned to the RIV

cell. The stage values for open-water bodies used in the steps described above were determined using a 10 m NED elevation model. The minimum value from the 10 m NED elevation model within the area of the water body was set as the stage.

As described in Section 4.2.4, the conductance of RIV boundary cells was adjusted during calibration by adjusting hydraulic conductivity values for lake/river bed sediments. Head values assigned to RIV boundary cells remains fixed during transient simulations.

3.6.6 High-Capacity Wells and Quarry Dewatering

Groundwater withdrawals for which there are water-use permit records maintained by the Minnesota Department of Natural Resources (DNR) through the State Water Use Data System (SWUDS) were included in the model. The DNR requires all users withdrawing more than 10,000 gallons of water per day or 1-million gallons per year to obtain a permit and submit monthly water use records. A total of 4,639 wells or quarry dewatering operations are simulated in the model. Within the eleven-county metropolitan area, there were 998 records in the SWUDS database for which the source aquifer or location of the well could not be determined. These withdrawals were not included in the model. The unaccounted pumping includes both currently active and inactive permits and accounts for between 1 percent and 5 percent of the total reported pumping on a monthly basis, averaging 2.4 percent for all available records (1988-2010).

Wells open to a single hydrostratigraphic unit were simulated using the standard well (WEL) package in MODFLOW. For wells screened in multiple aquifers and hence spanning multiple model layers, the Multi-Node Well (MNW2) package was used (Konikow and others, 2009). The MNW2 package automatically calculates the amount of water withdrawn from each contributing model layer. These rates are dependent on the aquifer properties (primarily transmissivity) and hydraulic gradients in contributing aquifers. The MNW package allows for more accurate simulation of wells pumping from multiple aquifers, even allowing the upper cells that a well penetrates to become dry and redistributing the total specified pumping rate to lower layers. These capabilities are not possible with the standard WEL package. The MNW2 package also allows for the transfer of water across confining units via open boreholes; something known to take place in the metro area but rarely quantified or simulated. For example, Runkel and others (2013) measured downward flow between the Jordan Sandstone and Tunnel City Group of approximately 60 gpm in a borehole in eastern Washington County. The MNW2 package can therefore act as both of sink and source of

groundwater to the aquifer system as water is transferred between layers via the borehole. In reported mass balance for the model, water flowing into a multi-aquifer well either due to pumping or a head difference across aquifer units is reported as an outflow. Water flowing from a multi-aquifer well into an aquifer due to borehole (inter-well) flow across aquifer units is reported as an inflow. Wells with positive pumping rates (injection wells) will also report as an inflow to the model, however there are no injection wells simulated in the model.

All wells within the model were initially identified by a concatenation of the County Well Index (CWI) unique ID, the DNR permit number, the DNR installation ID, and the DNR use code. This naming scheme was developed to allow for the use of the commonly used CWI unique IDs while still accommodating those wells that do not have a CWI unique ID listed in the SWUDS database. The use of the DNR permit number, installation ID, and use code was required to achieve a complete set of unique names (no duplicates). The following example demonstrates this naming system.

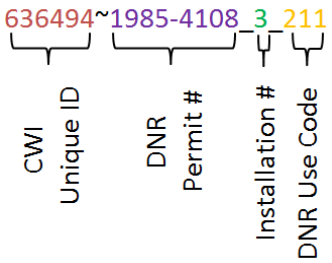

The CWI unique ID and the DNR permit number are always separated by a "~" sign. If the well does not have a CWI unique ID then the well name starts with a "~" sign. The DNR use code is always the last three integers. In the example above, the use code of "211" indicates that the well is used for municipal supply. The installation code of "3" indicates that it is the third well included in permit number 1985-4108. The CWI unique ID for this well is 636494, which can be used to look up additional well-construction data and drilling records in the CWI database.

Due to a limitation on the width of well names in the MNW2 package, well identifications for multi-aquifer wells had to be defined with shorter names than those described above. A lookup table relating the well names used by the MNW2 package and the identification system described above is provided in Appendix D. All single-aquifer wells using the WEL package maintain the longer identification scheme from above.

3.7 Solvers and Convergence Criteria

The NWT Solver (Niswonger and others, 2011) was used for this study. A head tolerance of $1.0x10^{-4}$ m and flux tolerance of 100 m^3/day were used for solver convergence criteria. Maximum outer iterations for the solver were 500. The portion of cell thickness used to smoothly adjust storage and conductance coefficients as the saturated thickness of a cell approaches zero was set at $1.0x10^{-4}$ m. All other solver settings were set at default values for "complex" problems as defined internally within the solver code.

4.0 Model Calibration

The term “calibration” as it refers to the Metro Model 3 is the process of adjusting the values of selected hydrologic model parameters within specified ranges in order to produce a good match between the model’s predictions of hydrologic indicators and previously observed conditions and measurements. A better term to describe this process is “history matching” or optimization. In this report, the term “calibration” is often used because it is familiar to those with experience in the use of groundwater-flow models. The term optimization is often used to describe results or components of the overall calibration process.

The MODFLOW model was calibrated through a series of automated inverse optimization procedures using the model-independent parameter estimating software BEOPEST (Version 13.0; Doherty, 2010b). Automated inverse optimization is a method for minimizing the differences, or residual, between simulated results and observations. The sum of the squared weighted residuals for all targets is the objective function that is to be minimized. The square of the residual is used because some residuals are negative and some are positive. BEOPEST is part of the PEST family of optimization software (Doherty 2010a; Doherty, 2013) and uses exactly the same optimization algorithms as PEST. The main difference between the two is that BEOPEST offers much greater flexibility in handling parallel run management (calibration on many machines or processors at once). For calibration of the Metro Model 3 up to 90 processors were used in parallel, and hence, BEOPEST was necessary for run management. Throughout this document PEST and BEOPEST may be referred to interchangeably as they both refer to the same algorithms and methods.

The overall process of the calibration procedure employed for this study was as follows:

1. The model was constructed.
2. Calibration targets were chosen.
3. Parameters that were allowed to vary during the calibration process were chosen, along with the range in which parameters were allowed to vary.
4. The results of the PEST optimization were evaluated and changes were made to the model;
    - the lower and upper bounds for parameter values were adjusted,
    - insensitive parameters were tied together or fixed, and/or

- the weights of observations were adjusted so that one type of observation does not influence the calibration too much, or observations that are less certain don't contribute excessively to the objective function.

5. Steps 4-5 were repeated numerous times to improve the optimization.

The groundwater-flow system in the Twin Cities metropolitan area is extremely complex (as are all natural systems) and what is known about this system originates from a very small number of ad hoc observations made over time. Furthermore, these observations have inherent uncertainty, both in value and in what they imply about how the flow system functions. There is a necessary trade-off between including model complexity (in the form of additional parameters that can be adjusted in the calibration process) and the very practical limits of computer resources, schedule, and budget. The calibration process involved making some choices on which parameters (e.g., hydraulic conductivity, river cell conductance, etc.) would be allowed to vary, the maximum and minimum values in which the parameter values could be varied, and initial estimates for the parameter values.

Some parameters are more correlated than others, which indicate that different combinations of some parameter values can produce nearly identical results. Thus, an optimized model may be too non-unique – which is not necessarily a desirable outcome. The use of more (and more varied) types of targets during calibration improves the optimization by reducing this non-uniqueness (Hill and Tiedeman, 2007). Also, placing constraints on the range a parameter can vary (i.e. upper and lower limits) can assist in reducing non-uniqueness. However, placing too much constraint on parameter limits can hinder the optimization process due to the need to vary the parameter values over large ranges in order to assess the numerical derivative. A common problem with automated calibration methods is insensitive parameters moving toward extreme values to achieve minimal progress in lowering the objective function. To overcome this issue Tikhonov regularization constraints were implemented (Doherty, 2003; Fienen et al, 2009; Tikhonov, 1963).

Part of the utility of this model is to suggest new locations and types of data that can be collected to better understand the flow system and reduce the model's predictive uncertainty. These new data will eventually suggest that the model be made even more complex than it currently is; not less. Undoubtedly, computational capabilities will continue to increase, as well, allowing for the inclusion of additional sensitive parameters.

4.1 Calibration Targets

Calibration targets were categorized into several different groups based on data-type, data-source, and data-accuracy. Residuals for each group were initially weighted based on the magnitude of the data. Unweighted residuals for baseflow will inherently be several magnitudes larger than unweighted residuals for hydraulic head, simply as a result of the units of measurement for each data type. Additionally, unweighted residuals for small streams will be lower than larger streams even if the relative percent errors are equal. Weights for each target group were adjusted so that individual target groups would not initially contribute disproportionally to the total objective function (Figure 22). As calibration progressed, if residuals from a target group began to contribute excessively to the objective function the weights were adjusted. Additional details regarding each target group are discussed below.

4.1.1 Hydraulic Head

Hydraulic head targets were derived from a number of different sources, all with varying levels of error. Head-target groups were established based on data sources, accuracy of data, and time period the data pertain to. Figures showing the spatial distribution of each head-target group are shown on Figures 23 to 30 and include:

- Minnesota DNR observation wells (ObWells) from 2003 to 2011
- USGS synoptic water-levels from March and August 2008 (Sanocki and others, 2009)
- White Bear Lake Synoptic Water Levels from 2011 (Jones et. al., 2013)
- Minnesota Pollution Control Agency (MPCA) Environmental Data Access (EDA) database and other water level data from miscellaneous monitoring wells (MPCA, 2013)
- USGS National Water Information System (NWIS) water levels 2003-2011
- USGS National Water Information System (NWIS) water levels prior to 2003
- County Well Index (CWI) static water levels 2003-2011
- County Well Index (CWI) static water levels prior 2003

For datasets that include a time series, or multiple water levels, the average of the observations was used for the target value for the steady-state calibration. These include: USGS synoptic water-levels from March and August 2008, White Bear Lake Synoptic Water Levels from 2011, and Minnesota DNR observation wells from 2003 to 2011. Additional

transient observations, expressed as head change, were included as separate calibration target groups and are discussed in Section 4.1.6.

Factors affecting the accuracy and precision of hydraulic head calibration targets vary significantly between datasets. Data compiled from the CWI are considered to have the most inherent error; however, CWI data covers the largest geographic extent. Data from synoptic water-level datasets, DNR observation wells, and other miscellaneous monitoring wells are considered to have the least amount of error. Obvious outliers in the CWI dataset, highlighted using cross-validation techniques, were removed from the calibration dataset. Additionally, outliers visually observed by plotting time series data were removed. Sources of error include the following:

- Inaccurate water-level measurement. Methods used to measure water levels vary widely. Water levels in CWI are often obtained by drilling contractors who may not have used precise measuring devices.
- Inaccurate well location. Many wells in the CWI database are identified only to the nearest quarter-quarter-quarter section, which may result in up to 600 feet of location error. Many other wells are located using GPS equipment, which can have accuracies as large as several meters to as small as several centimeters depending on the equipment used.
- Inaccurate elevation. The elevation of a measuring point (e.g. top of well casing, or ground surface) along with the depth to water is used to calculate the hydraulic head elevation. The accuracy of elevation data varies between datasets. Ground-surface elevations for CWI wells are typically estimated using 7.5-minute topographic maps. Standard practice assumes that elevations determined using topographic map contours have a measurement error of ½ the contour interval. Where topographic map contour intervals are 10 feet, measurement error is ±5 feet. Where well locations are inaccurate and areas of high slope, elevation estimates have even greater error. Most monitoring and observation wells are surveyed for elevation to accuracies ranging between ± 1 foot to ± 0.01 foot.
- Unstable water levels at the time of measurement. Water levels in the CWI were typically collected during or immediately after well installation or development and may not have reached equilibrium with the aquifer. Water levels from monitoring and observation wells represent more stable water levels.

- Misidentification or incorrect assignment of hydrostratigraphic units in databases. The well may actually be screened in a different unit, or in multiple units.
- Seasonal pumping affects on water levels. Depending on where the well is located and at what time of year it was installed, the water-level measured may have been affected by seasonal pumping. Where multiple measurements are available, the average water level is used as the steady-state model calibration target to help reduce this source of error. However, seasonal bias may still be present in wells with hundreds of measurements as those measurements may have consistently been measured in one season (e.g. not measured in the winter).
- Long-term changes in water levels due to climate or growing water demand. Water levels are affected by season and year of installation. For the steady-state calibration, water levels measured prior to the period represented by the model were grouped separately. The steady-state model uses average recharge and pumping from 2003-2011. Water levels measured prior to this period may represent a different condition than is being simulated, since regional pumping has generally increased over time with population growth.

All the different sources of error for water level measurements were considered in weighting target observations for the calibration process.

For hydraulic head calibration targets associated with wells screened in multiple hydrostratigraphic units (multi-aquifer wells), the simulated hydraulic head was calculated using the method proposed by Sokol (1963) and shown in Equation 4-1.

$$h_w = \frac{T_1 h_1 + T_2 h_2 + \cdots + T_n h_n}{T_1 + T_2 + \cdots + T_n} \qquad \text{Eqn. 4-1}$$

where:
h_w = simulated hydraulic head for the well
T = transmissivity of hydrostratigraphic unit (model layer)
h = hydraulic head for hydrostratigraphic unit (model layer)

4.1.2 Head Difference

For nested monitoring and observation wells the difference in hydraulic head between hydrostratigraphic units was used for calibration. Head-difference targets can help constrain the model calibration and often reduce model non-uniqueness and uncertainty by

maintaining the direction of vertical hydraulic gradients. These targets were only established at locations of nested wells where the accuracy of the measurements is less than the head difference between the two observations; hence, CWI observations are not applicable to this group.

4.1.3 Baseflow

Baseflow targets for different river reaches were established using baseflow separation of long term stream monitoring data. River gauges maintained by the USGS were analyzed using the software BFI (Wahl and Wahl, 1995; Wahl and Wahl, 2007). Other flow data were analyzed by the Metropolitan Council using WHAT (Web-based Hydrograph Analysis Tool) (Engel and Lim, 2004; Lim and others 2005). All baseflow calibration targets are summarized in Table 2. The simulated flux for each target reach was calculated using the River Observation Package (RVOB) of MODFLOW.

4.1.4 Transmissivity

Values of aquifer transmissivity determined from large-scale pumping tests, as compiled by Tipping and others (2010), were used as calibration targets to constrain the hydraulic conductivity distribution (Figure 31). While these targets influence the values at individual pilot points they are not directly associated or linked with individual pilot points. The final (bulk) hydraulic conductivity is a function of both the primary hydraulic conductivity, set with pilot points, and the secondary hydraulic conductivity, set with a depth dependent function (see Section 3.5.1). Bulk hydraulic conductivity and thickness of the open interval at each test well were used to calculate simulated transmissivity. For pumping tests conducted at wells open to multiple aquifers, composite transmissivity was calculated by summing the transmissivity of individual hydrostratigraphic units.

Table 2. Baseflow targets

Target Description	Target Name	Target Baseflow (m^3/day)	Target Baseflow (cfs)	Time Period Used	Primary Data Source and Gage Identification
Bevens Creek	Bevens_001	94,609	38.7	1989 to 2009	MCES (Bevens Creek 2)
Browns Creek	Browns_001	19,083	7.8	1989 to 2009	MCES (Browns Creek 0.3)
Cannon River above Cannon River at Welch, MN	Cannon_001	984,497	402	2003 to 2011	USGS (05355200)[a]
Carver Creek	Carver_001	55,048	22.5	1989 to 2009	MCES (Carver Creek 1.7)
Credit River	Credit_001	29,775	12.2	1989 to 2008	MCES (Credit River 0.6)
Crow River between edge of model and Rockford, MN	Crow_001	979,364	400	2003 to 2011	USGS (05280000)[b]
Elk River	Elk_Riv_001	370,605	151	2003 to 2011	USGS (05275000)[c]
High Island Creek	High_Is_001	96,954	39.6	2003 to 2010	USGS (05327000)
Minnesota River from edge of model to Jordan, MN	MN_Riv_001	743,500	304	2003 to 2011	USGS (05325000, 05330000)[d]
Minnesota River Between Jordan, MN and Fort Snelling State Park, MN	MN_Riv_002	1,181,400	483	2003 to 2011	USGS (05330000, 05330920)[e]
Mississippi River from edge of model to Anoka	Miss_Riv_001	2,146,087	877	2003 to 2011	USGS (05270700, 05288500, 05286000, 05280000, 05275000)[f]
Mississippi River between St. Paul, MN and Hastings, MN	Miss_Riv_002	293,100	120	2003 to 2010	USGS (05331000, 05331580)[g]
Nine Mile Creek	Nine_Mi_001	35,720	14.6	1989 to 2009	MCES (Nine Mile Creek 1.8)
Riley Creek	Riley_001	5,812	2.4	1999 to 2009	MCES (Riley Creek 1.3)
Rum River between edge of model and St. Francis, MN	Rum_Riv_001	471,912	193	2003 to 2011	USGS (05286000)[h]
Rum River between St. Francis and Rum River 0.7 gage	Rum_Riv_002	10,622	4.3	1996-2011	USGS (05286000), MCES (Rum River 0.7)[i]
Sand Creek upstream of 8.2 gage	Sand_Crk_001	189,610	77.5	1990 to 2009	MCES (Sand Creek 8.2)
St. Croix River between St. Croix Falls, WI and Mississippi River	St_Croix_001	1,545,400	632	2003 to 2011	USGS (05340500, 05344490)[j]
Valley Creek	Vly_Crk_001	31,781	13.0	1990 to 2009	MCES (Valley Creek 1)
Vermillion River upstream of Empire, MN	Vermil_001	117,660	48.1	2003 to 2010	USGS (05345000)

[a] Mean baseflow for Cannon River at Welch (560 cfs) less baseflow of Straight River new Fairbault (158 cfs)

[b] Mean baseflow for Crow River at Rockford of 852 cfs scaled based on contributing area that is within the model domain (47%).

[c] Mean baseflow for Elk River near Big Lake of 216 cfs scaled based on contributing area that is within the model domain (70 %)

[d] Difference between average baseflow at Jordan, MN (5068 cfs) and average baseflow at Mankato, MN (4615 cfs) scaled based on percent contributing area within the model domain (67%). Model calculated flux includes the flux for contributing tributaries (Bevens Creek, High Island Creek, Le Sueur Creek, Rush River)

[e] Difference between average baseflow at Jordan, MN (5068 cfs) and average baseflow at Fort Snelling, MN (5629 cfs) less average combined discharge from Blue Lake and Seneca wastewater discharge (77.9 cfs). Data from Fort Snelling based on annual mean discharge of 8,673 cfs with a calculated BFI of 0.649 from 2003 to 2010. Model flux includes the flux from contributing tributaries (Assumption Creek, Carver Creek, Credit River, Eagle Creek, Nine Mile Creek, Purgatory Creek, Riley Creek, Sand Creek)

[f] Difference between average baseflow at Anoka (7137 cfs) and average baseflow at St. Cloud (4,670 cfs) less average baseflow for gaged tributaries; Rum River at St. Francis, MN (521 cfs), Crow River at Rockford, MN (852 cfs), and Elk River near Big Lake, MN (216 cfs). Model flux includes flux from gaged tributaries downstream of gages and also includes all or portions of Briggs Creek, Clearwater River, Fairhaven Creek, Johnson Creek, Luxemburg Creek, Robinson Hill Creek, Snake River, St Francis River, Thiel Creek, and Three Miler Creek.

[g] Difference between average baseflow for Mississippi River at Hastings, MN (11,813 cfs) and average baseflow for Mississippi River at St. Paul, MN (11,391 cfs) less waste water discharge from Metro Plant (281.9 cfs), Eagle Point Plant (5.6 cfs), and Empire Plant (14.7 cfs). Data for Mississippi River at Hastings, MN only includes 2003, and 2007 to 2010. Waste water discharge from Empire Plant to Mississippi River began in March 2008

[h] Average baseflow for Rum River at St. Francis, MN (521 cfs) scaled based on percent of contributing area is within model domain (37%).

[i] Average baseflow for Rum River at 0.7 from 1996 to 2009 (564.9 cfs) less average baseflow for Rum River at St. Francis for 2003-2011 of (521.32 cfs).

[j] Average baseflow for St. Croix River at St. Croix Falls, WI for 2003 to 2011 (3167.60 cfs) less average baseflow for St. Croix River at Prescott for 2008,2010,2011 (4,249.41 cfs) less average waste water discharge from St. Croix Valley plant (4.8 cfs) and less approximate tributary flow not in model: Kinnickinnic River near River Falls, WI (95.63 cfs), Willow River at Willow River State Park (101.90 cfs), and Apple River (247.03 cfs) near Somerset, WI. Model calculated flux includes tributary flux within the model (Browns Creek, Falls Creek, Lawrence Creek, Old Mill Stream, Valley Creek)

4.1.5 Flow Direction

Groundwater-flow direction targets were established by defining flow directions based on the axis of mapped plumes of groundwater contamination (Metropolitan Council, 2012). A total of 16 flow direction targets were established (Figure 32). Flow direction targets were not established for small plumes where it was not evident what the prominent regional flow direction is based on the plume migration. Modeled flow directions for each target were calculated by using three simulated hydraulic head values around the axis of the target. The three head values were then used to solve a three-point problem (Fienen, 2005) to calculate the simulated flow direction.

4.1.6 Transient Hydraulic Head Change (Drawdown)

Head-change targets were established for USGS synoptic water levels from March and August 2008, White Bear Lake area synoptic water levels from 2011, and Minnesota DNR observation wells from 2003 to 2011. For each location, or well, head change was calculated using the first observation occurring during the time period of the transient simulation as the reference head. For example, head change for a USGS synoptic water-level measurement for August 2008 was calculated as March 2008 water level minus August 2008 water level. Many of the MN DNR observation wells have time-series data recorded as frequently as once every 15 minutes. The transient model cannot capture this level of detail due to constraints of monthly stress periods with weekly time steps. Hydraulic head data from these wells were resampled to average weekly values prior to establishing head change targets.

4.1.7 Relative Flux Constraints

Targets for the relative flux into or out of boundary conditions were established to help control the mass balance on the model and also used to help constrain model conceptualization. Actual flux values for these targets are not known but are rather estimated based on qualitative data. Including these target values imposes constraints to better match the conceptual model.

A potentially significant source of water to the groundwater-flow system is derived from leakage out of lakes, which are simulated using river cells (RIV Package). Based on the results of the SWB model (Metropolitan Council, 2012), the average surface runoff from

2003 to 2011 was 1.45 in/year over the model domain. This equates to 5% of precipitation (rain and snowmelt); infiltration accounts for 26%, and evapotranspiration accounts for 69% of precipitation. These percentages are comparable to those estimated by Sanford and Selnick (2012). Of the 1.45 in/year that runs off across the model domain, some leaves the system via surface-water flow in the Mississippi River; the rest flows into lakes where it either evaporates, is stored within the lake basin, or infiltrates into the groundwater system. The amount that infiltrates from lakes is unknown. However, it is assumed to be less than 50% of the total runoff. A relative flux constraint was established so that if flux into the groundwater model from all lakes equates to a volume greater than 0.725 in/year (50% of 1.45 in/year) a residual, or "penalty", is applied to the target observation. If the flux into the model from all lakes is less than 0.725 in/year no residual is applied.

The Vermillion River between the town of Vermillion, Minnesota and Vermillion Falls in Hastings, Minnesota is recognized as a losing stream reach. The volume of water lost to the groundwater system is unknown due to limited measurements over the time period of model calibration. A relative flux constraint was used for this stretch of the river. If the river along the stretch was gaining, a residual or penalty was applied; if the river was losing (supplying water to the groundwater system) no penalty or residual was applied.

Baseflow of the Mississippi River between USGS gages at Anoka, Minnesota and St. Paul, Minnesota is unknown. Analysis of baseflow separation data for these two gauges, along with the Minnesota River at Fort Snelling, results in inconclusive results that are within the expected error of the stream gages (5%). This stretch of the river is highly controlled by locks and dams and there are a number of large water withdrawals and discharges that compound the difficulty in estimating baseflow. While a true baseflow estimate for this stretch of river is unknown available data indicate that it is at least 200 cubic feet per second (cfs) A relative flux target was established where a residual or "penalty" is applied if baseflow is less than 200 cfs.

4.2 Parameters for Optimization

Parameters for optimization were categorized into several different groups. These include:

- Horizontal and vertical hydraulic conductivity of each bedrock hydrostratigraphic unit
- Horizontal and vertical hydraulic conductivity of Quaternary materials
- Infiltration/recharge parameters
- River/lake conductance (bed hydraulic conductivity)
- Parameters associated with bedrock hydraulic conductivity depth-dependent function
- Storage (specific storage and specific yield) for each bedrock hydrostratigraphic unit and Quaternary materials
- Quasi-3D confining bed hydraulic conductivity

Grouping parameters into different groups allows for regularization to be adjusted and applied differently for each parameter type/group and also allows for more detailed examination of the sensitivity of different types of parameters. Additional details regarding parameters used for optimization are discussed below.

4.2.1 Hydraulic Conductivity of Bedrock Hydrostratigraphic Units

As described in Section 3.5.1 and illustrated on Figure 18 the bulk hydraulic conductivity values of bedrock units were parameterized in the model using a combination of pilot points (to estimate the primary hydraulic conductivity) and a depth-dependent function (to account for secondary hydraulic conductivity where hydrostratigraphic units are near the bedrock surface). Values of primary horizontal hydraulic conductivity and vertical anisotropy at each pilot point location were used as adjustable parameters during calibration. Vertical anisotropy was used to help constrain values of vertical hydraulic conductivity to be less than values of horizontal hydraulic conductivity. Vertical anisotropy and horizontal hydraulic conductivity values were used to generate vertical hydraulic conductivity parameter values for MODFLOW. Additionally, for each bedrock hydrostratigraphic unit, constants C and λ of the depth-dependent function (Eqn. 3-1) described in Section 3.5.1 were adjustable parameters during calibration.

4.2.2 Hydraulic Conductivity of Quaternary, Glenwood, Platteville, and Decorah Hydrostratigraphic Units

Methods used to calculate the effective hydraulic conductivity for model cells that represent the Quaternary sediments, Glenwood, Platteville, and Decorah hydrostratigraphic units are

described in Section 3.5.2. The horizontal and vertical hydraulic conductivity values of each material type (e.g., sand, clay, Platteville Formation) were used as adjustable parameters for model calibration. Additionally, the large areas of Quaternary sediments mapped as "unknown" by Tipping (2011) were subdivided into hydraulic conductivity zones. The horizontal and vertical hydraulic conductivity of "unknown" Quaternary sediments in each of these zones were also used as adjustable parameters. The extent of each zone representing unknown Quaternary sediments was determined by a combination of surficial geology, thickness of unknown sediments, bedrock valleys, and extent of exiting stratigraphy models/mapped areas where sediments are already well defined (e.g. northwest metro area). (Figure 33).

4.2.3 Hydraulic Conductivity of Quasi-3D Confining Units

As described in Section 3.3.1 quasi-3D layers are used to represent the confining characteristics of the base of the St. Peter Sandstone, Prairie du Chien Group, and Tunnel City Group, where present. The vertical hydraulic conductivity of each of these quasi-3D confining units was an adjustable parameter for calibration. The actual value of the vertical hydraulic conductivity has little real-world meaning as it is only used to adjust the conductance of the confining beds. As described in Section 3.3.1 each quasi-3D confining layer is set at a constant thickness of 0.1 meters and does not represent the actual thickness of confining beds.

4.2.4 Lake-bed and stream-bed conductance

The conductance of river (RIV) boundary cells is expressed as:

$$C = \frac{KA}{M} \quad \text{(Eqn. 4-2)}$$

Where:
C = conductance of RIV boundary for cell
K = hydraulic conductivity of the riverbed or lakebed
A = area of the river or lake that intersects the cell
M = thickness of the riverbed or lakebed sediments

For purposes of model calibration the hydraulic conductivity of the lake/riverbed sediments was used as an adjustable parameter for calculating RIV cell conductance; the thickness of the riverbed or lakebed sediments was assumed to be equal to one meter. Lakes were categorized into 19 different groups, based on surficial geology shown on Figure 34 (Hobbs and Goebel, 1982). The hydraulic conductivity of lakebed sediments for each group was

adjusted as part of the calibration process. The hydraulic conductivity of riverbed sediments for each major river was adjusted as part of the calibration process. In some instances, larger rivers were subdivided into several reaches (Figure 35). The relative distribution of initial parameter values for lake hydraulic conductivity were set based on surficial geology; lakes in till set with lower initial conductance than lakes in sand. Initial parameter values for rivers was assumed higher than lakes and generally set at 1 m/day. These initial relative distributions were not strictly enforced during calibration as there is little data to constrain them.

4.2.5 Storage

Similar to primary hydraulic conductivity, the specific yield (the storage parameter for unconfined conditions in aquifers) and the specific storage (the storage parameter for confined conditions in aquifers) at each pilot-point location were adjustable during calibration. Specific-yield values for units that are confined throughout the entire model domain (e.g. Mount Simon – Hinckley, Eau Claire) were fixed during calibration as the model is insensitive to specific yield where a unit is confined.

4.2.6 Infiltration

Infiltration, as calculated using the Soil-Water Balance (SWB) Model (Metropolitan Council, 2012; Westenbroek et. al., 2010), was used to define the initial distribution of infiltration across the entire model domain. Sensitivity analysis of SWB input parameters and uncertainty analysis of SWB calculated infiltration from Metropolitan Council (2012; Appendix A) were used to guide how infiltration could vary during calibration of the groundwater-flow model.

The mean (μ) and standard deviation (σ) of infiltration for each of the land-use soil type combinations from Metropolitan Council (2012) were used to develop scaling factors, or multipliers, for each combination of land use and soil type (Table 3; Figures 36 and 37). These scaling factors represent the range of infiltration and accounts for uncertainty of the most sensitive parameters in the SWB model. It is common for the allowed range for a parameter's value in a model calibration to represent the 95-percent confidence interval (for example, see Doherty, 2011 pp. 12 and 199). Consequently, the values $(\mu - 1.96\ \sigma)/\mu$ and $(\mu + 1.96\ \sigma)/\mu$ were used to establish the scaling factors for each combination of land use and soil type. These scaling factors are designed to allow infiltration to vary during

calibration of the groundwater-flow model while keeping the infiltration within expected ranges and tied to the uncertainty, which can vary across the model domain.

Table 3. Range of recharge scaling factors

Land Use	A Soils Min. | Max	B Soils Min. | Max	C Soils Min. | Max	D Soils Min. | Max
Open Water	1.00 | 1.00	1.00 | 1.00	1.00 | 1.00	1.00 | 1.00
Low Density Residential	0.80 | 1.20	0.90 | 1.10	0.99 | 1.01	0.66 | 1.34
High Density Residential	0.73 | 1.27	0.91 | 1.09	0.98 | 1.02	0.74 | 1.26
Commercial / Industrial / Transient	0.78 | 1.22	0.01 | 1.99	0.89 | 1.11	0.67 | 1.33
Bare Rock / Sand	1.00 | 1.01	0.99 | 1.01	1.00 | 1.00	0.85 | 1.15
Quarries / Pits	0.97 | 1.03	0.63 | 1.37	0.99 | 1.01	0.83 | 1.17
Deciduous Forest	0.98 | 1.02	0.78 | 1.22	0.99 | 1.01	0.63 | 1.37
Evergreen Forest	0.99 | 1.01	0.99 | 1.01	0.99 | 1.01	0.62 | 1.38
Mixed Forest	1.00 | 1.00	1.00 | 1.00	0.99 | 1.01	0.61 | 1.39
Shrub Land	0.77 | 1.23	0.89 | 1.11	1.00 | 1.00	0.66 | 1.34
Grass / Herbs	0.85 | 1.15	1.00 | 1.00	0.99 | 1.01	0.71 | 1.29
Pastures	1.00 | 1.01	1.00 | 1.00	0.99 | 1.01	0.64 | 1.36
Row Crops	1.00 | 1.00	0.79 | 1.21	1.00 | 1.00	0.75 | 1.25
Urban / Recreational Grass	0.85 | 1.15	0.90 | 1.10	0.99 | 1.01	0.62 | 1.38
Wetlands	0.99 | 1.01	0.99 | 1.01	0.99 | 1.01	0.60 | 1.41

4.3 Regularization

Tikhonov regularization constraints (Tikhonov, 1963; Doherty, 2003; Fienen and others, 2009) were used to keep parameters near a preferred central value and limit differences between parameters of the same group unless significant improvement could be achieved in lowering the objective function. Regularization is implemented with PEST by simultaneously evaluating the "measurement-objective function" which is quantified by the level of model fit to traditional target values (hydraulic head, baseflow, etc.) and a "regularization-objective function" which is quantified by the level of model fit to regularization constraints (targets) that represent a preferred condition. The weight applied to regularization constraints is gradually reduced during the calibration process.

Regularization constraints, commonly referred to as "preferred-difference constraints", were used exclusively. For each combination of hydraulic conductivity and storage parameters within each hydrostratigraphic unit, a preferred difference was specified as 0. For example, the difference between the parameter value at one pilot point location for the Jordan Sandstone and all other pilot points within the Jordan Sandstone was preferred to be at a

value of 0. If values of 0 were achieved for all constraints in a given hydrostratigraphic unit, a homogeneous aquifer would be simulated.

Similar preferred-difference constraints were used for all infiltration multiplier values. For example, the preferred difference between the multiplier applied for row-crops with B soils and the multiplier for all other land-use soil-type combinations was specified as 0. These constraints result in a preferred state where all recharge multipliers for each land-use soil-type combination are the same.

4.4 Optimization Results

4.4.1 Model Fit

Model fit was evaluated using several different calibration statistics along with visual comparison of measurements to simulated model results. Residuals used in calculating statistics were defined in the same way as calculated by PEST:

$$residual = measured - simulated$$

Calculating residuals as defined above results in somewhat counterintuitive residual signs. Negative residuals indicate that the model-simulated values are greater than measured values and positive residuals indicate that the model-simulated values are less than measured values.

Table 4 summarizes the calibration statistics for hydraulic-head calibration targets across the different target groups. The residual mean measures the average tendency of simulated values to be greater (negative residual mean) or less than measured values (positive residual mean). The residual mean for all hydraulic-head targets was -3.64 meters and ranged from 0.78 meters to -3.83 meters for individual head-target groups. The absolute residual mean is the average of the absolute value of the residuals. The absolute residual mean for all targets was 5.30 meters and ranged from 2.14 meters to 6.02 meters for individual head-target groups.

The root mean square error (RMSE) is the square-root of the average of the squared residuals. RMSE is a model-calibration statistic that is generally more sensitive to outliers than other model-calibration statistics and gives a better sense of the range of residuals. The RMSE for all hydraulic-head targets was 7.89 meters, and ranged from 2.70 meters to 8.51 meters for individual head-target groups. RSME is often compared to the ranges in

measurements; a small value for the ratio of RMSE to the range of measured values (typically less than 0.1) indicates good overall model fit (Spitz and Moreno, 1996). The ratio of RSME to the range in measurements was 0.04 for all head targets and ranged from 0.04 to 0.07 for individual target groups.

Table 4 Summary of hydraulic head calibration statistics

Target Group[a]	Residual Mean (m)	Absolute Residual Mean (m)	Root Mean Square Error (RMSE) (m)	Ratio of RMSE to Measurement Range
All Head Targets	-3.64	5.30	7.89	0.04
MN DNR ObWells	-1.63	5.26	8.51	0.05
USGS 2008 Synoptic	-3.83	6.02	8.30	0.06
USGS 2011 White Bear Lake Synoptic	-0.66	2.14	3.29	0.04
Misc. Monitoring Wells	-1.07	2.31	2.70	0.04
CWI 2003 to 2011	-3.47	5.07	7.56	0.04
CWI pre-2003	-3.70	5.35	7.96	0.04
NWIS 2003 to 2011	0.78	2.98	5.19	0.06
NWIS pre-2003	-2.52	5.36	7.98	0.07

[a] Refer to section 4.1 for description of target groups

Plots showing measured versus simulated hydraulic-head targets are show on Figures 38 to 46.

Measured and simulated baseflows and calculated residuals are presented in Table 5 and on Figure 47. For a few reaches, particularly small streams in southern Hennepin and Carver Counties, simulated and measured baseflow values do not agree, suggesting an area for improvement in conceptualization, parameterization, and/or model design. It may be that the scale of the model is not able to accurately capture the flow system controlling baseflow to these smaller streams. The percent difference between measured and simulated baseflow is relatively high for some larger river reaches (e.g. Minnesota River north of Jordan), however, the error in the measured values for these reaches is very high and was reflected in the weights assigned to these observations.

Table 5 Summary of measured and simulated baseflow statistics

River Reach	Measured (m^3/day)	Simulated (m^3/day)	Residual (m^3/day)	Percent Difference
Bevens Creek	-94,609	-11,590	-83,019	156
Browns Creek	-19,083	-17,669	-1,414	8
Cannon River above Cannon River at Welch, MN	-984,497	-1,276,760	292,263	26
Carver Creek	-55,048	-12,964	-42,084	124
Credit River	-29,775	-32,004	2,229	7
Crow River between edge of model and Rockford, MN	-979,364	-409,655	-569,709	82
Elm Creek	-39,012	-37,846	-1,167	3
Elk River	-370,605	-438,565	67,960	17
High Island Creek	-96,954	-35,947	-61,007	92
Mississippi River from edge of model to Anoka	-2,146,087	-1,467,640	-678,447	38
Mississippi River between St. Paul, MN and Hastings, MN	-293,100	-375,698	82,598	25
Minnesota River from edge of model to Jordan, MN	-743,500	-907,555	164,055	20
Minnesota River Between Jordan, MN and Fort Snelling State Park, MN	-1,181,400	-487,318	-694,082	83
Nine Mile Creek	-35,720	-23,425	-12,295	42
Riley Creek	-5,812	468	-6,280	170
Rum River between edge of model and St. Francis, MN	-471,912	-433,547	-38,365	8
Rum River between St. Francis and Rum River 0.7 gage	-106,622	-125,299	18,677	16
Sand Creek upstream of 8.2 gage	-189,610	-14,791	-17,4820	171
St. Croix River between St. Croix Falls, WI and Mississippi River	-1,545,400	-710,697	-834,703	74
Vermillion River upstream of Empire, MN	-117,660	-54,441	-63,219	73
Valley Creek	-31,781	-22,229	-9,552	35
White Bear Lake	14,950	9,516	5,434	44

The values of transmissivity calculated from pumping tests across the metro area were used as observations (i.e. “measured” transmissivity). During the optimization process, the transmissivities at these pumping test locations were calculated from the values of hydraulic conductivity (multiplied by saturated thickness), which were adjustable parameters at the pilot points locations. The residual (i.e. difference) between the “measured” transmissivity values and the model-calculated values contributed to the overall objective function and PEST attempted to minimize these residuals in the context of the overall optimization process.

Simulated transmissivity at the pumping test locations was typically less than the “measured” transmissivity (Figure 48). This bias may be a result of several factors. Tight regularization controls on bedrock hydraulic conductivity pilot points and the relatively small

number of pilot points used may have hindered the calibration process from achieving a better match with measured transmissivity. Also, "measured" transmissivity values are the products of analytical calculations that employ severely limiting assumptions such as an infinite areal aquifer extent and are themselves subject to considerable uncertainty. "Measured" values may actually be biased high due to inaccurately accounting for leakage in the analysis of aquifer tests and wells often being sighted in more productive zones of an aquifer. Results are presented using both the open-interval and model-layer thickness to calculate simulated transmissivity; during calibration, the open-interval thickness was used.

"Measured" groundwater-flow directions were used as calibration targets, even though flow direction is not a directly measured observation. As discussed, several "measured" groundwater flow direction targets were calculated for known contaminant plumes using hydraulic-head measurements and the three-point method of vector calculation. Groundwater-flow directions were included in the optimization process because these directions (as manifested by the development of a dissolved contaminant plume from a known source area) are indicators of regional groundwater-flow conditions. In many cases, the model's predictions of groundwater-flow direction would likely be similar to the "measured" flow direction even without using flow direction as a target but including them as targets provides an additional constraint on the model's parameter values. "Measured" flow directions are compared to simulated flow directions on Figure 49. The mean residual for flow direction targets was 12.5 degrees. Flow direction target FlwDir07 has a large disagreement between measured and simulated directions. This target is associated with a contaminant plume in northeastern Dakota County. Flow directions associated with this plume are known to be influenced by highly localized geologic features that are not captured at the scale of the model (Barr Engineering, 1998)

Measured versus simulated head change for the period 2007 to 2011 is shown on Figure 50. Overall, trends in drawdown are well-represented. However, at extreme head change the model tends to slightly over-estimate head change, while for smaller head change the model tends to simulate slightly less change. Comparison of USGS synoptic head-change measurements between March 2008 (a low groundwater demand period) and August 2008 (a high groundwater demand period) are shown on Figure 51 through 53. The overall trends for large seasonal cones of depression are well-represented. Most discrepancies between USGS's interpreted change and the model's simulated change are in areas where measurements or pumping data are lacking. USGS data indicate an area of drawdown of

more than 25 feet in far southeast Washington County while the model simulated no drawdown in this area. Further review indicates that a high capacity irrigation well that was actively pumping during the summer of 2008 is located near the center of this cone of depression. However, this well has no geologic record or aquifer information associated with it as was not included in the model (see Section 3.6.6). Inclusion of this well (in the proper aquifer) would likely remedy this discrepancy. USGS interpolations used the natural-neighbor interpolation scheme, which may result in larger cones of depression in areas not constrained by actual measurements. In some areas, particularly in the Mt Simon-Hinckley aquifer, areas interpreted by the USGS as one large cone of depression are simulated by the model as several more-focused cones of depression around pumping centers. Additionally, areas of high pumping not represented in the measured dataset show larger drawdowns. Also noted is the large drawdown in the Tunnel City and Wonewoc aquifers in western Dakota, southern Hennepin, and western Washington Counties. These areas lack measurements and were interpolated by the USGS as having little change. The model predicts large drawdowns in the Tunnel City and Wonewoc aquifers, primarily driven by high pumping in the overlying Prairie du Chien and Jordan aquifers. The drawdown in the Tunnel City and Wonewoc aquifers below these large pumping centers indicates a leakage connection between the aquifer units. Further verifying and understanding this connection and resolving discrepancies on the extent of cone(s) of depression in the Mount Simon-Hinckley aquifer will likely require more comprehensive monitoring in the future.

4.4.2 Estimated Parameter Values

The spatial distribution of hydraulic conductivity values for each bedrock hydrostratigraphic unit as a result of the model calibration process are shown on Figures 54 through 74. Additionally, resulting values for the arithmetic mean, geometric mean, minimum, maximum, depth function λ, and depth function C values for each bedrock hydrostratigraphic unit are shown. Values of individual pilot points are labeled on the figures for reference. However, the values of the individual pilot points do not include the application of the depth dependent function as discussed in Section 3.5.1. Values shown with color flooding on the figures of spatially distributed hydraulic conductivity values represent the calibrated values used by the model.

The spatial distribution of calibrated hydraulic conductivity values for Quaternary sediments in each model layer are shown on Figure 75 through 92. These values represent effective

hydraulic conductivity calculated using methods discussed in Section 3.5.2. Values of individual Quaternary material types used to calculate effective hydraulic conductivity are shown in Table 6. Additionally, values of Quaternary zones where the depositional materials are unknown are shown on Figure 93 and 94. Hydraulic conductivity values for Quaternary material types in Table 6 are generally greater than those presented by Tipping (2011). This is typical of hydraulic conductivity, where values typically increases with the scale of the measurement (Schulze-Makuch and others, 1999) and is particularly true for very heterogeneous media such as Quaternary sediments.

Table 6. Quaternary material hydraulic conductivity values

Quaternary Material Type	Horizontal Hydraulic Conductivity (m/day)	Vertical Hydraulic Conductivity (m/day)
Sand and Gravel	2.4E+01	7.6E+00
Fine Sand	1.2E+01	6.8E-01
Loam to Sandy Loam	8.3E+00	2.8E-01
Loam to Sandy Clay Loam	7.5E+00	1.9E-01
Sandy Silt	1.8E+00	2.5E-02
Loam to Sandy Loam - Deep	1.6E+00	1.5E-02
Loam to Sandy Clay Loam - Deep	1.4E+00	1.3E-02
Loam, Silt Rich; Silt and Clay	1.3E+00	1.2E-02
Loam to Clay Loam	7.8E-01	1.1E-02
Loam, Silt Rich; Silt and Clay - Deep	6.2E-01	1.5E-04
Loam to Clay Loam	5.6E-01	1.4E-04

Note: "Deep" indicates unit is more than 60 feet below ground surface

River and lake conductance values for the calibrated model, expressed as values of vertical hydraulic conductivity of river/lake bed sediments, assuming a bed thickness of one meter, are shown in Figure 95.

The spatial distribution of calibrated storage values (specific storage and specific yield), for each bedrock hydrostratigraphic unit, are shown on Figures 96 through 110. Storage values for Quaternary sediments are shown on Figures 111 through 128. Additionally, the arithmetic mean, geometric mean, minimum, and maximum values are shown on these figures. Values of individual pilot points are labeled on the figures for reference.

As discussed in Section 4.2.6 infiltration, as calculated using the Soil-Water Balance (SWB) Model (Metropolitan Council, 2012; Westenbroek et. al., 2010), was used to define the initial distribution of infiltration across the entire model domain. The mean (μ) and standard deviation (σ) of infiltration for each of the land-use soil type combinations from Metropolitan Council (2012) were used to develop scaling factors, or multipliers, for each combination of

land use and soil type These scaling factors are designed to allow infiltration to vary during calibration of the groundwater-flow model while keeping the infiltration within expected ranges and tied to the uncertainty, which can vary across the model domain. Recharge multipliers for the calibrated model are in Table 7.

Table 7. Recharge multipliers

Land Use	A Soils	B Soils	C Soils	D Soils
Open Water	1.00	1.00	1.00	1.00
Low Density Residential	0.80	0.90	1.00	1.34
High Density Residential	0.76	1.09	1.00	1.03
Commercial / Industrial / Transient	0.78	0.69	1.10	1.11
Bare Rock / Sand	1.00	1.00	1.00	1.00
Quarries / Pits	1.00	1.37	1.00	0.99
Deciduous Forest	1.00	0.78	1.00	0.66
Evergreen Forest	1.00	1.00	1.00	0.94
Mixed Forest	1.00	1.00	1.00	0.99
Shrub Land	0.81	0.91	1.00	0.95
Grass / Herbs	0.85	1.00	1.00	0.99
Pastures	1.00	1.00	1.00	0.64
Row Crops	1.00	0.79	1.00	0.75
Urban / Recreational Grass	0.85	1.10	1.00	1.12
Wetlands	1.00	1.00	1.00	0.62

4.5 Parameter Sensitivity

Output from PEST can be used to facilitate calculation of the sensitivities of each weighted observation with respect to each parameter. PEST calculates the composite sensitivity of each parameter with respect to all observations based on Equation 4.3.

$$s_i = \frac{1}{m}\left(\sum_{k=1}^{m}\left(\frac{\partial o_k}{\partial p_i} w_k\right)^2\right)^{1/2} \qquad \text{(Eq. 4.3)}$$

where:

s_i is the composite sensitivity for the i^{th} parameter (p_i)

m is the number of observations

$\partial o_k / \partial p_i$ is the partial derivative of the k^{th} observation with respect to the i^{th} parameter

w_k is the weight assigned to the k^{th} observation

Composite sensitivities were calculated for each parameter based on all of the observations included in the calibration, excluding regularization information. Parameter sensitivities were grouped and ranked in several ways; each offering different insight into the relative importance of individual parameters or parameter groups.

Ranking the composite sensitivity of individual parameters demonstrates which parameters are most sensitive to all observation targets. The 50 most sensitive parameters are shown on Figure 129. The most sensitive individual parameter was the recharge multiplier for row-crops with B soils, followed by horizontal hydraulic conductivity pilot point Number 2 for the Prairie du Chien Group, and horizontal hydraulic conductivity for Quaternary sands. The sensitivity of individual parameters is highly dependent on the number of observations near, or influenced by, a parameter. For example, the recharge multiplier for row crops with B soils and horizontal hydraulic conductivity of Quaternary sands both rank high as individual parameters because they each have an effect on large areas of the model domain and therefore, influence many observations. Also, Prairie du Chien pilot point Number 2 is located in east-central Hennepin County, an area with a large number of observations.

Ranking parameter groups by contribution to the summed composite sensitivity offers additional insight. While the single most sensitive parameter is the recharge multiplier for row-crops with B soils, the recharge multiplier group ranks fourth when considering its contribution to the summed composite sensitivity; the horizontal hydraulic conductivity for bedrock parameter group ranks first (Figure 129). Four parameter groups; horizontal hydraulic conductivity of bedrock, quaternary vertical hydraulic conductivity, Quaternary horizontal hydraulic conductivity, and the recharge multiplier, contribute to over 80 percent of the summed composite sensitivity. However, the sum of composite sensitivities is highly influenced by the number of parameters in a parameter group; larger number of parameters typically results in a larger contribution to the summed composite sensitivity.

Normalizing the sum of parameter sensitivities for each group by the by number of parameters in the group highlights parameter groups with relatively high average sensitivity (Figure 129). The bedrock depth function *C* parameter group only has twelve parameters but each is relatively sensitive. Similarly, the quasi-3D confining-bed vertical hydraulic conductivity group has only three parameters but each is relatively sensitive, particularly for the quasi-3D layers representing the basal St. Peter and Oneota confining beds.

Additional plots showing the most sensitive parameters in each parameter group are presented in Appendix B.

4.6 Mass Balance

The inflows and outflow for the model are presented in Table 8 and in Figure 130.

Table 8a. Summary of model mass balance- Unsaturated Zone

Budget Component		Cubic meters per day
Inflow: Infiltration		10,905,524
Total Unsaturated Zone Inflow	*10,905,524*	
Outflow: UZF Recharge		9,358,057
Outflow: Reduced/Rejected Infiltration		1,547,467
Total Unsaturated Zone Outflow	*10,905,524*	
Percent Discrepancy Unsaturated Zone	**0.0%**	

Table 8b. Summary of model mass balance- Saturated Zone

Budget Component		Cubic meters per day
Inflow: Recharge		9,358,110
Inflow: Seepage from surface waters		3,084,930
Inflow: Constant head boundaries		388,866
Inflow: General head boundaries		130,680
Inflow: Wellbore flow (MNW)		218,231
Total Saturated Zone Inflow	*13,180,817*	
Outflow: Baseflow / seepage to surface waters		11,349,878
Outflow: Single aquifer wells		718,520
Outflow: Constant head boundaries		82,932
Outflow: General head boundaries		43,353
Outflow: Multi-aquifer wells (MNW)		986,078
Total Saturated Zone Outflow	*13,180,761*	
Percent Discrepancy Unsaturated Zone	**0.0%**	

Not surprisingly, recharge by infiltrating precipitation is by far the largest source of water to the groundwater flow system. Leakage from rivers and lakes contributes most of the remaining source component of the mass balance. Constant-head and general-head boundaries provide very little water to the flow system, suggesting that the areal extent of the model encompasses nearly all of the hydraulic sources. Nearly all of the groundwater in the model domain is predicted to discharge to rivers. Wells are the other main discharge sink. Inflow via wellbore flow from multi-aquifer wells occurs due head differences between aquifers connected through an open well. Flow into the well is reported as an outflow and

flow out of the well into a different aquifer is reported as an inflow. See section 3.6.6 for additional discussion. The mass balance of the overall model is essentially zero.

5.0 1995-2011 Transient Simulation

In order to assess the ability of the Metro Model 3 to simulate longer term transient response to pumping and recharge, a simulation representing 1995 through 2011 was developed.

Similar to the shorter transient-simulation, an initial steady-state stress-period was used to define starting heads, followed by monthly transient stress-periods, each with four time steps. Average pumping and recharge for 1990 through1994 was used for the initial steady-state stress period. Also, similar to the shorter transient-simulation, a simple two-layer model was used to simulate the time lag between infiltration and recharge. The only difference compared to the method described in Section 3.6.1 is the that period 1988 through1994 was simulated twice prior to simulating the period 1995 to 2011 to make sure that the soil moisture characteristics were properly developed leading into to the simulation of January 1995.

Changes in hydraulic head at the location of each DNR observation well were tracked using the first observation occurring during the time period of the transient simulation as the reference head. Simulated change in hydraulic head compared to measured change is shown on Figure 131. Overall, the longer transient simulation does a slightly better job at capturing the change in hydraulic head compared to the shorter transient simulation. Time-series plots comparing simulated and measured change in hydraulic head for each of the 337 wells tracked during the simulation are presented in Appendix C.

The simulated change in hydraulic head in the Prairie du Chien-Jordan aquifer for three period intervals: August 1995 and August 2000; August 1995 and August 2005; and August 1995 and August 2010 is shown on Figure 132. An area of hydraulic head rebound (rise in hydraulic head) (shown as Area A in Figure 132) is evident in east Hennepin County and west-central Anoka County. These rebounds are primarily caused by converting once-through cooling systems in and around the core cities to cooling methods that don't consume as much groundwater. In Area A of Figure 132, 73 percent of the total pumping reduction between August 1995 and August 2010 is from reduction in groundwater use by once-through cooling systems. In other areas, particularly those areas that experienced population growth in the late 1990's and early 2000's cones of depression (lower hydraulic head) are evident. Pumping from the Prairie du Chien – Jordan aquifer for an area in

northwest Dakota County (Area B on Figure 132) has increased since 1995, particularly in the summer months, resulting in increased drawdown.

Plot of simulated change in hydraulic head for the Mt. Simon-Hinckley aquifer for similar time periods is shown on Figure 133. As with the Prairie du Chien-Jordan aquifer, an area of hydraulic head rebound is evident for the Mt. Simon-Hinckley aquifer in east Hennepin County and west-central Anoka County (Area A in Figure 133). Pumping in this area from the Mt. Simon-Hinckley aquifer has decreased since 1995, likely in response to a moratorium on the use of the Mt. Simon-Hinckley aquifer in the seven-county metro area. Outer suburban areas show cones of depression in the aquifer during this period. However, these cones of depression do not appear to be growing at a consistent rate, but rather are dependent on the year-to-year pumping from the aquifer, particularly in the summer months. Some municipalities only pump from the Mt. Simon-Hinckley aquifer when absolutely necessary and may pump very little from the aquifer during wetter summers.

6.0 Use and limitations of the model

The model described in this report was designed, conceptualized, and calibrated as a regional groundwater-flow model. It is intended to be used as a tool to guide regional planning, inform the Master Water Supply Plan, and assess potential impacts associated with changes in regional pumping and/or land-use change. In order to interpret the results of predictive scenarios, users must understand both the uncertainty in the numerical groundwater model as well as uncertainty in water demand and land use projections. The large scale, regional nature of the model cannot be over-emphasized. While the model may prove useful for smaller scale studies (particularly for defining boundary conditions), further evaluation of the model in the specific area of interest should be conducted prior to using the model to make any conclusions about aquifer conditions, response, fluxes, flow directions, or water levels. Some guidance on implementing additional hydrogeologic data, and refining the model grid for local studies is provided in a supplemental user manual associated with this report (Metropolitan Council, 2014), but it is ultimately the user's responsibility to assess the appropriateness of the model for the desired use and to verify that the data, parameter values, boundary conditions, and conceptualization in this model are correct for their use.

The model described in this report is the third iteration of a regional flow model for the Twin Cities metropolitan area. Each iteration has incorporated new data, implemented new and more powerful software, and has been conceptualized slightly differently as our understanding of the hydrogeologic system in the Twin Cities area continues to evolve. The ability to accurately simulate groundwater flow in the area is dependent on high quality data to develop and calibrate the model. If you use this model, or associated data, for additional study it would be appreciated if any new data generated can be shared with the Metropolitan Council for use in any future iterations of this model. Additional feedback is also always welcome.

7.0 References

Anderman, E.R., and Hill, M.C., 2000, MODFLOW-2000, the U.S. Geological Survey modular ground-water model Documentation of the Hydrogeologic-Unit Flow (HUF) Package: U.S. Geological Survey Open-File Report 2000-342, 89 p.

Anderson, J.R., Runkel, A.C., Tipping, R.G., Barr, K., D.L., and Alexander, E.C., Jr., 2011, Hydrostratigraphy of a fractured, urban, aquitard: in Miller, J.D., Jr., Hudak, G.J., Tittkop, C., and McLaughlin, P.I., eds, Archean to Anthropocene: Field Guides to the Geology of the Mid-Continent of North America: Geological Society of America Field Guide 24, 457-475

Anderson, M.P. and W.W. Woessner, 1992. Applied Groundwater Modeling, Simulation of Flow and Advective Transport. Academic Press, Inc., New York, New York, 381 p

Austin, G.S., 1969. Paleozoic lithostratigraphic nomenclature for southeastern Minnesota: Minnesota Geological Survey Information Circular 6, 11p.

Barr Engineering, 1998. Technical Memorandum, Hydrogeologic Conceptual Model, Kock Refinery Groundwater Risk Evaluation/Corrective Measures Study, Prepared for Koch Refining Co. September, 1998.

Barr Engineering, 2008. Background and methodology for the recharge input to the Twin Cities Metro Groundwater Model. Appendix A in Metropolitan Council, 2009, Draft Twin Cities Metropolitan Area Regional Groundwater Flow Model Version 2.00, technical report in support of the Metropolitan Area Master Water Supply Plan.

Barr Engineering, 2010. Evaluation of groundwater and surface-water interaction: guidance for resources assessment, Twin Cities metropolitan area, Minnesota. Prepared for Metropolitan Council, June 2010. 27p. plus GIS files.

Bauer, E.J. 2009. Geologic Atlas of Carver County, Minnesota. Minnesota Geological Survey County Atlas Series C-21.

Brooks, R H, and A. T. Corey. 1964. Hydraulic properties of porous media. Hydrology Papers, Colorado State University

Cohen, P., 1963. Specific-yield and particle-size relations of Quaternary alluvium in the Humboldt River Valley, Nevada, USGS Water-Supply Paper 1669-M, 23 p.

Delin, G.N. and D.G. Woodward. 1984. Hydrogeologic Setting and the Potentiometric Surfaces of Regional Aquifers in the Hollandale Embayment, Southeastern Minnesota, 1970-80. USGS Water Supply Paper 2219. 56 p.

Doherty, J., 2003, Groundwater model calibration using pilot-points and regularization: Ground Water, v. 41, no. 2, p. 170–177

Doherty, J.E., Fienen, M.N., and Hunt, R.J., 2010, Approaches to highly parameterized inversion: Pilot-point theory, guidelines, and research directions: U.S. Geological Survey Scientific Investigations Report 2010–5168, 36 p

Doherty, J., 2010a, PEST, Model-independent parameter estimation—User manual, 5th ed.: Brisbane, Australia, Watermark Numerical Computing

Doherty, J., 2010b, Windows BEOPEST. Watermark Numerical Computing

Doherty, J., 2013, Addendum to the PEST manual: Brisbane, Australia, Watermark Numerical Computing

Dripps W.R. and K.R. Bradbury. 2007. A simple daily soil-water balance model for estimating the spatial and temporal distribution of groundwater recharge in temperate humid areas. Hydrogeology Journal 15, 433-444

Engel, B.A, K.J. Lim. 2004. WHAT website. Accessed June, July, August 2010 at: http://cobweb.ecn.purdue.edu/~what/

Environmental Simulations, Inc., 2011. Guide to using Groundwater Vistas, Version 6, Environmental Simulations Inc.

Fienen, M.N., Muffels, C.T., and Hunt, R.J., 2009, On constraining pilot point calibration with regularization in PEST: Ground Water, v. 47, no. 6, p. 835–844

Feinstein, D.T., Hunt, R.J., and Reeves, H.W. 2010. Regional groundwater-flow model of the Lake Michigan Basin in support of great lakes basin water availability and use studies. USGS Scientific Investigations Report 2010-5109.

Fienen, M.N., 2005. The three-point problem, vector analysis and extension to the n-point problem. Journal of Geoscience Education, v. 53, n. 3, p. 257-262

Hansen, D.D. and J.K. Seaberg. 2000. Metropolitan Area Groundwater Model Project Summary – Lower Aquifers Model Layers 4 and 5; Ver. 1.00.

Harbaugh, A.W., 2005, MODFLOW-2005, The U.S. Geological Survey modular ground-water model—the Ground-Water Flow Process: U.S. Geological Survey Techniques and Methods 6-A16, variously p.

Hill, M.C., 1990. Preconditioned Conjugate-Gradient 2 (PCG2), A Computer Program for Solving Ground-Water Flow Equations. U.S. Geological Survey Water-Resources Investigations Report 90-4048, Denver, Colorado, 43p.

Hill, M.C. and C.R. Tiedman. 2007. Effective groundwater model calibration: with analysis of data, sensitivities, predictions, and uncertainty, New Jersey, John Wiley & Sones, Inc., 455p.

Hobbs, H.C. and J.E., Goebel, 1982. Geologic map of Minnesota, Quaternary geology: Minnesota Geological Survey, State Map Series S-01, scale 1:500,000.

Jirsa, M.A., T.J. Boerboom, V.W. Chandler, J.H. Mossler, A.C. Runkel, and D.R. Setterholm. 2011. Geologic map of Minnesota: Minnesota Geological Survey, State Map Series S-21, bedrock geology, scale 1:500,000.

Johnson, A.I., 1963. Specific yield; compilation of specific yields for various materials, USGS OFR 63-59 C1, 119 p.

Johnson, M.D., and H.D. Mooers. 1998. Ice-margin positions of the Superior lobe during Late Wisconsinan deglaciation. in Patterson, C.J., and H.E. Wright eds. Contributions to Quaternary studies in Minnesota: Minnesota Geological Survey Report of Investigations 49, p. 7-14.

Jones, P.M., Trost, J.J., Rosenberry, D.O., Jackson, P.R., Bode, J.A., and O'Grady, R.M., 2013. Groundwater and surface-water interactions near White Bear Lake, Minnesota, through 2011: U.S. Geological Survey Scientific Investigations Report 2013-5044, 73p.

Juckem, P. 2009. Simulation of the Groundwater-Flow in Pierce, Polk, and St. Croix Counties, Wisconsin. United States Geological Survey Scientific Investigations Report 2009-5056.

Kanivetsky, R., 1978. Hydrogeologic map of Minnesota: Bedrock Hydrogeology. Minnesota Geological Survey Map Series, S-2.

Konikow, L.F., Hornberger, G.Z., Halford, K.J., and Hanson, R.T., 2009, Revised multi-node well (MNW2) package for MODFLOW ground-water flow model: U.S. Geological Survey Techniques and Methods 6–A30, 67 p.

Lim, K.J., B. A. Engel, Z. Tang, J. Choi, K.S. Kim, S. Muthukrishnan, and D. Tripathy. 2005. Automated web GIS based hydrograph analysis tool, WHAT. Journal of the American Water Resources Association 42 (6): 1407-1416

Lorenz, D.L. and Delin, G.N. 2007. A regression model to estimate regional groundwater recharge. Ground Water, 45, no. 2, p196-208.

McDonald, M.G. and Harbaugh, A.W., 1988. A modular three-dimensional finite-difference ground-water flow model: U.S. Geological Survey Techniques of Water-Resources Investigations, Book 6, chap. A1, 586 p.

Metropolitan Council. 2009. Twin Cities Metropolitan Area Regional Groundwater Flow Model Version 2.00. technical report in support of the Metropolitan Area Master Water Supply Plan, October 2009.

Metropolitan Council. 2011. DEMs: top surfaces of bedrock units in Goodhue, Rice, Le Sueur, and Isanti Counties. Unpublished data.

Metropolitan Council, 2012. Groundwater contamination plumes Unpublished data

Metropolitan Council, 2012. Using the soil water balance model (SWB) to estimate recharge for the Twin Cities Metropolitan Area Groundwater Model Version 3. Prepared by Barr Engineering. Metropolitan Council: Saint Paul, MN.

Metropolitan Council, 2014. Metro Model 3 User Manual and Tutorial Guide. Prepared by Barr Engineering. Metropolitan Council: Saint Paul, MN.

Minnesota Department of Natural Resources. 1998. Part B of the Geologic Atlas of Stearns County, Minnesota. County Atlas Series C-10, Part B.

Minnesota Geological Survey. 1995. Part A of the Geologic Atlas of Stearns County, Minnesota. County Atlas Series C-10, Part A.

Minnesota Geological Survey. 1996. Text Supplement to the Geologic Atlas of Stearns County, Minnesota. County Atlas Series C-10, Part C.

Minnesota Geological Survey. 2006b. Geologic Atlas of Scott County, Minnesota. County Atlas Series C-17.

Minnesota Geological Survey. 2009. Geologic Atlas of McLeod County, Minnesota. County Atlas Series C-20.

Minnesota Geological Survey. 2010. Geologic Atlas of Chisago County, Minnesota. County Atlas Series C-22.

Minnesota Geological Survey. 2011. Geologic Atlas of Sibley County, Minnesota. County Atlas Series C-24.

Minnesota Pollution Control Agency (MPCA), 2013, Environmental Data Access. Accessed from: http://www.pca.state.mn.us/index.php/data/environmental-data-access.html

Mossler, J.H. 2005a. Bedrock geology of the Stillwater quadrangle, Washington County, Minnesota: Minnesota Geological Survey Miscellaneous Map M-153, scale 1:24,000.

Mossler, J.H. 2005b. Bedrock geology of the Hudson quadrangle, Washington County, Minnesota: Minnesota Geological Survey Miscellaneous Map M-154, scale 1:24,000.

Mossler, J.H. 2005c. Bedrock geology of the St. Paul Park quadrangle, Washington and Dakota counties, Minnesota: Minnesota Geological Survey Miscellaneous Map M-166, scale 1:24,000.

Mossler, J.H. 2006a. Bedrock geology of the St. Paul Park quadrangle, Washington and Dakota counties, Minnesota: Minnesota Geological Survey Miscellaneous Map M-166, scale 1:24,000.

Mossler, J.H. 2006b. Bedrock geology of the Prescott quadrangle, Washington and Dakota counties, Minnesota: Minnesota Geological Survey Miscellaneous Map M-167, scale 1:24,000.

Mossler, J.H. 2006c. Bedrock geology of the Vermillion quadrangle, Dakota County, Minnesota: Minnesota Geological Survey Miscellaneous Map M-168, scale 1:24,000.

Mossler, J.H. 2006d. Bedrock geology of the Hastings quadrangle, Dakota, Goodhue, and Washington counties, Minnesota: Minnesota Geological Survey Miscellaneous Map M-169, scale 1:24,000.

Mossler, J.H. 2008. Paleozoic Stratigraphic Nomenclature for Minnesota. Minnesota Geological Survey Report of Investigations 65.

Mossler, J.H. 2011. Bedrock Geology, pl. 2 of Meyer, G.N., Geologic Atlas of Anoka County, Minnesota: Minnesota Geological Survey County Atlas C-27, scale 1:100,000.

Mossler J.H., and V.W. Chandler. 2009. Bedrock geology, pl. 2 of Bauer, E.J., project manager, Geologic Atlas of Carver County, Minnesota: Minnesota Geological Survey County Atlas C-21, 6 pls., scale 1:100,000.

Mossler J.H. and V.W. Chandler. 2011a. Bedrock geology, pl. 2 of Geologic Atlas of Nicollet County, Minnesota: Minnesota Geological Survey County Atlas C-25, scale 1:100,000.

Mossler J.H. and V.W. Chandler. 2011b. Bedrock geology, pl. 2 of Geologic Atlas of Sibley County, Minnesota: Minnesota Geological Survey County Atlas C-24, scale 1:100,000.

Mossler, J.H. and R.G. Tipping. 2000. Bedrock geology and structure of the seven-county Twin Cities metropolitan area, Minnesota. Minnesota Geological Survey Miscellaneous Map Series M-104.

Niswonger, R.G., Prudic, D.E., and Regan, R.S., 2006. Documentation of the unsaturated-Zone Flow (UZF1) Package for modeling unsaturated flow between the land surface and the water table with MODFLOW-2005: U.S. Geological Survey Techniques and Methods 6-A19, 62p.

Niswonger, R.G., Panday, S., Ibaraki, M., 2011. MODFLOW-NWT, A Newton formulation for MODFLOW-2005: U.S. Geological Survery Techniques and Methods 6-A37, 44 p.

Norvitch, R. F., Ross, T. G., and Brietkrietz, Alex, 1973, Water-resources outlook for the Minneapolis-St. Paul metropolitan area: Metropolitan Council of the Twin Cities.

Olsen W. 2008. Geologic contact models for Dakota County (excluding the Hastings area). Dakota County Water Resources Department. acquired via email from William Olsen on 5/14/2012.

Rawls, W. J., Brakensiek, D. L., & Saxton, K. E. 1982. Estimation of soil water properties. Trans. Asae, 25(5), 1316-1320.

Runkel, A.C., R.Tipping, P. Jones, J. Meyer, B. Parker, E.C. Alexander, J. Steenberg. A. 2013. Multilevel monitoring system provides new insights into bedrock aquitard in southeastern Minnesota, Presented at Minnesota Groundwater Association Conference, April, 2013.

Runkel, A.C. and T.J. Boerboom. 2010. Bedrock geology, pl. 2. of Geologic Atlas of Chisago County, Minnesota: Minnesota Geological Survey County Atlas C-22, scale 1:100,000.

Runkel, A.C., Tipping, R.G., Alexander, E.C. Jr., Green, J.A., Mossler, J.H., and Alexander, S.C.. 2003a. Hydrogeology of the Paleozoic Bedrock in Southeastern Minnesota. Minnesota Geological Survey Report of Investigations 61.

Runkel, A.C., R.G. Tipping, and J.H. Mossler. 2003b. Geology in support of groundwater management for the northwestern Twin Cities Metropolitan Area. Final report to the University of Minnesota and the Metropolitan Council, August 27, 2003.

Runkel, A.C., and Tipping R.G. 2006. Bedrock topography, depth to bedrock, and bedrock geology models, pl. 5 of Setterholm, D.R., Geologic Atlas of Scott County, Minnesota: Minnesota Geological Survey County Atlas C-17.

Runkel, A.C., J.H. Mossler, R.G. Tipping, and E.J. Bauer. 2006. A hydrogeologic and mapping investigation of the St. Lawrence Formation in the Twin Cities Metropolitan Area. Minnesota Geological Survey Open File Report 06-04.

Runkel A.C., and J.H. Mossler. 2006. Bedrock geology, pl. 2 of Setterholm, D.R., Geologic Atlas of Scott County, Minnesota: Minnesota Geological Survey County Atlas C-17.

Runkel, A.C., J.R. Steenberg, and R.G. Tipping. 2011. Hydraulic conductivity and hydrostratigraphy of the Platteville Formation, Twin Cities metropolitan area, Minnesota. Minnesota Geological Survey report submitted to the Metropolitan Council, November, 2011.

Sanford, W.E. and Selnick, D.L, 2012. Estimation of evapotranspiration across the conterminous United States using a regression with climate and land-cover data. Journal of American Water Resources Association (JAWA) V. 49, no. 1, p. 217-230.

Sanocki, C.A., Langer, S.K., and Menard J.C. 2009. Potentiometric surfaces and changes in groundwater levels in selected bedrock aquifers in the Twin Cities Metropolitan Area, March-August 2008 and 1988-2008: U.S. Geological Survey Scientific Investigations Report 2009-5226, 67 p. with appendices.

Schoenberg, M.E. and J.H. Guswa. 1982. Evaluating ground-water data by a flow model of the Twin Cities metropolitan area, Minnesota. EOS, Transactions, American Geophysical Union, v. 63, no. 33, p. 612.

Schulze-Makuch, D., Carlson, D.S., & Malik, P. 1999. Scale dependency of hydraulic conductivity in heterogeneous media. Ground Water, 37(6), 904-919.

Smith, R.E., 1983. Approximate sediment water movement by kinematic characteristics: Soil Science Society of America Journal, v. 47, p 3-8.

Smith, R.E., and Hebbert, R.H.B., 1983. Mathematical simulation of interdependent surface and subsurface hydrologic processes: Water Resources Research, v. 19, no. 4, p. 987-1001.

Sokol, D., 1963. Position and Fluctuations of water level in wells perforated in more than one aquifer: Journal of Geophysical Research, V. 68, no. 4, p. 1079-1080.

Spitz, K. and Moreno, J. 1996. A practical guide to groundwater flow and solute transport modeling: New York, John Wiley and Sons, 426p.)

Streitz, A.R. 2003. Preparation of supporting databases for the Metropolitan Area Groundwater Model, Version 1.00. http://www.pca.state.mn.us/water/groundwater/mm-datareport.pdf. 45 p.

Thornthwaite C.W. 1948. An approach toward a rational classification of climate. Geog. Rev. 38: no.1, 55-94

Thornthwaite C.W. and J.R. Mather. 1957. Instructions and tables for computing potential evapotranspiration and the water balance. Publications in Climatology. 10: no. 3.

Tikhonov, A.N., 1963a, Solution of incorrectly formulated problems and the regularization method: Soviet Math. Dokl., v. 4, p. 1035–1038.

Tipping, R.G., A.C. Runkel, C.M. Gonzalez. 2010. Geologic investigation for portions of the Twin Cities Metropolitan Area: I. Quaternary/Bedrock Hydraulic Conductivity. II. Groundwater Chemistry, Metropolitan Council Water Supply Master Plan Development.

Tipping, R.G. 2011. Distribution of vertical recharge to upper bedrock aquifers, Twin Cities metropolitan area. Minnesota Geological Survey report submitted to Metropolitan Council, November, 2011.

Tipping, R.G. and Mossler, J.H. 1996. Digital elevation models for the tops of the St. Peter Sandstone, Prairie du Chien Group, Jordan Sandstone and St. Lawrence/St. Lawrence Formations within the seven-county metropolitan area: Minnesota Geological Survey, unpublished manuscript maps, scale 1:100,000, four digital files.

U.S. Geological Survey. 2009. National Elevation Dataset (NED), 1/3 arc-second resolution, http://nationalmap.gov.

U.S. Geological Survey, 2012, National Water Information System data available on the World Wide Web (USGS Water Data for the Nation), accessed at http://waterdata.usgs.gov/nwis/

Wahl, K. L., and Wahl, T. L., 1995. Determining the Flow of Comal Springs at New Braunfels, Texas,Texas Water '95, American Society of Civil Engineers, August 16-17, 1995, San Antonio, Texas, pp. 77-86.

Wahl, T.L. and K.L Wahl, 2007. BFI: A computer program for determining an index to base flow, version 4.15. Accessed at http://www.usbr.gov/pmts/hydraulics_lab/twahl/bfi/index.html

Westenbroek, S.M., Kelson, V.A., Dripps, W.R., Hunt, R.J., and Bradbury,K.R., 2010, SWB–A modified Thornthwaite-Mather Soil Water Balance code for estimating ground-water recharge: U.S. Geological Survey Techniques and Methods 6-A31, 60 p. The Soil Water Balance code is available for from the USGS at: http://pubs.usgs.gov/tm/tm6-a31/

Young, H.L. 1992. Hydrogeology of the Cambrian-Ordovician Aquifer System in the Northern Midwest, United States, U.S. Geological Survey Professional Paper 1405-B

www.barr.com
askbarr@barr.com

4700 West 77th Street
Minneapolis, MN
55435-4803

952.832-2600
Fax 952.832.2601

public.info@metc.state.mn.us
metrocouncil.org

390 Robert Street North
St. Paul, MN 55101-1805

651.602.1000
TTY 651.291.0904